

1 **Monitoring of carbon dioxide fluxes in a subalpine**  
2 **grassland ecosystem of the Italian Alps using a**  
3 **multispectral sensor**

4

5 **K. Sakowska<sup>1,2</sup>, L. Vescovo<sup>1</sup>, B. Marcolla<sup>1</sup>, R. Juszczak<sup>2</sup>, J. Olejnik<sup>2,3</sup>,**  
6 **D. Gianelle<sup>1,4</sup>**

7 [1]{Sustainable Agro-Ecosystems and Bioresources Department, Research and Innovation  
8 Centre - Fondazione Edmund Mach, Via E. Mach 1, 38010 - S. Michele all'Adige (TN),  
9 Italy}

10 [2]{Meteorology Department - Poznan University of Life Sciences, Piatkowska Street 94, 60-  
11 649 Poznan, Poland}

12 [3] {Department of Matter and Energy Fluxes, Global Change Research Center, AS CR, v.v.i.  
13 Belidla 986/4a, 603 00 Brno, Czech Republic }

14 [4] {Foxlab Joint CNR-FEM Initiative, Via E. Mach 1, 38010 - S.Michele all'Adige (TN),  
15 Italy}

16 Correspondence to: K. Sakowska (karolina.sakowska@fmach.it)

17

18 **Abstract**

19 The study investigates the potential of a commercially available proximal sensing system -  
20 based on a 16-band multispectral sensor - for monitoring mean midday gross ecosystem  
21 production ( $GEP_m$ ) in a dynamic subalpine grassland ecosystem of the Italian Alps equipped  
22 with an eddy covariance flux tower. Reflectance observations were collected for five  
23 consecutive years, characterized by different climatic conditions, together with turbulent  
24 carbon dioxide fluxes and their meteorological drivers. Different models based on linear  
25 regression (vegetation indices approach) and on multiple regression (reflectance approach)  
26 were tested to estimate  $GEP_m$  from optical data. The overall performance of this relatively  
27 low-cost system was positive. Chlorophyll-related indices including the red-edge part of the  
28 spectrum in their formulation (Red-Edge Normalized Difference Vegetation Index,  $NDVI_{red-}$

1  $_{\text{edge}}$ ; Chlorophyll Index,  $\text{CI}_{\text{red-edge}}$ ) were the best predictors of  $\text{GEP}_m$ , explaining most of its  
2 variability during the observation period. The use of the reflectance approach did not lead to  
3 considerably improved results in estimating  $\text{GEP}_m$ : the adjusted  $R^2$  ( $\text{adj}R^2$ ) of the model based  
4 on linear regression - including all the 5 years - was 0.74, while the  $\text{adj}R^2$  for the multiple  
5 regression model was 0.79. Incorporating mean midday photosynthetically active radiation  
6 ( $\text{PAR}_m$ ) into the model resulted in a general decrease in the accuracy of estimates,  
7 highlighting the complexity of the  $\text{GEP}_m$  response to incident radiation. In fact, significantly  
8 higher photosynthesis rates were observed under diffuse as regards to direct radiation  
9 conditions. The models which were observed to perform best were then used to test the  
10 potential of optical data for  $\text{GEP}_m$  gap-filling. Artificial gaps of three different lengths (1, 3  
11 and 5 observation days) were introduced in the  $\text{GEP}_m$  time series. The values of  $\text{adj}R^2$  for the  
12 three gap-filling scenarios showed that the accuracy of the gap filling slightly decreased with  
13 gap length. However, on average, the  $\text{GEP}_m$  gaps were filled with an accuracy of 73% with  
14 the model fed with  $\text{NDVI}_{\text{red-edge}}$ , and of 76% with the model using reflectance at 681, 720 and  
15 781 nm and  $\text{PAR}_m$  data.

## 16 **1 Introduction**

17 In recent years, quantifying and understanding the dynamics and the main drivers of  
18 ecosystem carbon exchange, as well as up-scaling the level of observations, have become  
19 critical challenges for the environmental scientific community (Canadell et al., 2000; Gamon  
20 et al., 2006; Running et al., 1999; Wohlfahrt et al., 2010).

21 The eddy covariance (EC) technique is a widely and commonly applied method to estimate  
22 carbon exchange between vegetation and the atmosphere at the ecosystem scale (Baldocchi,  
23 2003; Burba, 2013; Geider et al., 2001). Although this method is able to provide direct, near-  
24 continuous and high-temporal resolution measurements of net gas exchange, it also has some  
25 limitations.

26 EC technique provides flux measurements of a relatively small area. The flux “footprint”  
27 varies from tens of meters to several kilometers and depends on many parameters such as  
28 measurement height, wind velocity, surface roughness and atmospheric stability (Baldocchi,  
29 2003; Kljun et al., 2001; Schmid, 1994). At the same time, the EC systems are relatively  
30 expensive - a typical cost for a complete EC system is on the order of \$40 to \$50k (US), and  
31 the cost of site infrastructure is additional (Running et al., 1999). Considering all of these  
32 aspects, it is clear that, although EC measurements can be considered a solid basis for the

1 ecosystem scale CO<sub>2</sub> flux measurements, complementary methods are needed to extend the  
2 estimates to landscape and regional scales.

3 Important networks such as SpecNet, IMECC, and EUROSPEC have been investigating the  
4 potential of coupling spectral and EC observations (Balzarolo et al., 2011). In-situ  
5 measurements can provide unique datasets with high spectral, spatial and temporal resolution,  
6 which represent a solid basis for validation of remote observations carried out at aircraft and  
7 satellite levels and further up-scaling (Gamon et al., 2006; Gamon et al. 2010). As a result the  
8 number of sites where direct flux measurements are conducted simultaneously with in-situ  
9 spectral measurements have increased significantly within the last decade.

10 The most commonly used approach to estimate the gross ecosystem production (GEP;  $\mu\text{mol}$   
11  $\text{m}^{-2} \text{s}^{-1}$ ) with proximal sensing is based on the Light-Use Efficiency (LUE) model proposed  
12 by Monteith (Monteith and Moss, 1977; Monteith, 1972). This simple model assumes that  
13 GEP is driven by the Absorbed Photosynthetically Active Radiation (APAR;  $\mu\text{mol m}^{-2} \text{s}^{-1}$ )  
14 and the photosynthetic radiation use efficiency expressing the carbon sequestration efficiency  
15 per amount of the absorbed solar energy ( $\epsilon$ ;  $\mu\text{mol CO}_2 \mu\text{mol}^{-1} \text{APAR}$ ):

$$16 \quad \text{GEP} = \epsilon \cdot \text{APAR} = \epsilon \cdot f_{\text{APAR}} \cdot \text{PAR} \quad (1)$$

17 where PAR is the incident photosynthetically active radiation ( $\mu\text{mol m}^{-2} \text{s}^{-1}$ ) and  $f_{\text{APAR}}$  is the  
18 fraction of PAR absorbed by the vegetation canopy (%).

19 Numerous studies have highlighted that spectral vegetation indices (VIs) are a non-direct  
20 measure of canopy “greenness”, which is a complex parameter comprising a whole range of  
21 vegetation properties such as  $f_{\text{APAR}}$  (Inoue et al., 2008; Myneni and Williams, 1994; Sims et  
22 al., 2006; Walter-Shea et al., 1997), leaf area index - LAI (Gitelson et al., 2003c; Rossini et  
23 al., 2012; Serrano et al., 2000; Stenberg et al., 2004; Vescovo and Gianelle, 2008; Viña et al.,  
24 2011), chlorophyll content (Gitelson et al., 2005; Rossini et al., 2012; Wu et al., 2008), green  
25 herbage ratio (Gianelle and Vescovo, 2007; Vescovo and Gianelle, 2006) and fractional  
26 vegetation cover (Carlson and Ripley, 1997; Glenn et al., 2008).

27 In non-stressed ecosystems characterized by strong seasonal dynamics such as some managed  
28 croplands, independent estimates of  $\epsilon$  may be unnecessary due to its relation with the  
29 chlorophyll content (Gitelson et al., 2012; Peng and Gitelson, 2012; Peng et al., 2011;  
30 Rossini et al., 2012; Wu et al., 2009), and this is particularly true when integrating GEP over  
31 longer time scales, e.g. days (Gitelson et al., 2008). Therefore most of the variations in plant

1 productivity in such ecosystems should be reflected by changes in APAR (Lobell et al.,  
2 2002).

3 Several studies modelled GEP as a function of VIs (Harris and Dash, 2010; Rossini et al.,  
4 2010; Sims et al., 2006; Sjöström et al., 2009; Xiao et al., 2004) and/or of VIs multiplied by  
5 PAR (Gitelson et al., 2006; Peng and Gitelson, 2012; Peng et al., 2011). Including PAR in the  
6 model should theoretically enhance the correlation with GEP, because the product of VI and  
7 PAR takes into account the seasonal changes in both biophysical parameters controlling the  
8 photosynthesis process (e.g.  $f_{APAR}$  and chlorophyll content) and in the amount of radiation  
9 reaching the vegetation surface (Gitelson et al., 2012).

10 In the current study, five years of field multispectral data acquired with the Cropscan  
11 MSR16R system (Cropscan Inc., Rochester, USA) deployed on the EC tower of the  
12 FLUXNET grassland site IT-MBo (Viote del Monte Bondone, Trento, Italy) are presented  
13 and analyzed.

14 In particular, the objectives of this paper are:

15 i) to investigate the potential of vegetation reflectance and narrow-band VIs for  
16 monitoring carbon dioxide fluxes exchanged between the dynamic grassland ecosystem and  
17 the atmosphere;

18 ii) to analyze the relationships between spectral data and carbon dioxide fluxes during  
19 the five years of observations in order to determine how robust the relationships between  
20 vegetation spectral properties (reflectance and narrow-band VIs) and mean midday GEP  
21 ( $GEP_m$ ) are;

22 iii) to compare different approaches (correlation analysis and multiple regression) to  
23 estimate  $GEP_m$ ;

24 iiiii) to evaluate the potential of spectral models to gap-fill  $GEP_m$  data.

25

## 26 **2 Materials and methods**

### 27 **2.1 Experimental site**

28 The study site is a permanent alpine grassland located at 1550 m a.s.l. on the Viote del Monte  
29 Bondone plateau (46°00' N, 11°02' E, Italian Alps).

30 The vegetation of the area is dominated by *Festuca rubra* (L.) (covering 25% of the area),  
31 *Nardus stricta* (L.) (13%) and *Trifolium sp.* (L.) (14.5%), and is representative of a typical

1 low productive meadow of the alpine region. The site is managed as an extensive meadow  
2 with low mineral fertilization (applied in autumn) and is cut once a year, usually in mid-July  
3 (Gianelle et al., 2009). The maximum canopy height at the peak of the growing season (mid-  
4 June to early July) can reach approximately 30 cm.

5 The climate of this area is sub-continental (warm and wet summer) and is characterized by a  
6 mean annual temperature of 5.5 °C, with monthly averages ranging from -3.1 °C in February  
7 to 14.3 °C in July. The annual mean precipitation is 1244 mm, with maximum values in May  
8 (138 mm) and October (162 mm). The snow-free period lasts typically from early May to late  
9 October (Marcolla et al., 2011).

10 The site is characterized by a regular East-West wind circulation, showing along this direction  
11 an almost flat topography with a homogeneous vegetated fetch of more than 500 m. An  
12 experimental footprint analysis demonstrated that 30% (in stable atmospheric conditions) to  
13 80% (in unstable conditions) of the total CO<sub>2</sub> flux originates within 30 m from the EC tower  
14 (Marcolla and Cescatti, 2005).

## 15 **2.2 Eddy covariance and meteorological data**

16 Continuous EC measurements of CO<sub>2</sub>, water vapor and sensible heat fluxes were performed at  
17 the Monte Bondone FLUXNET site from the beginning of August 2002. In the present study,  
18 data from 2008 to 2012 were used, to match the available spectral dataset.

19 The Eddy Covariance (EC) system consisted of a Licor Li-7500 open-path infrared gas  
20 analyzer (Li-COR Inc., Lincoln, Nebraska, USA) and a Gill R3 3-D ultrasonic anemometer  
21 (Gill Instruments Ltd., Lymington, UK), mounted at a height of 2.5 m. Raw data were  
22 recorded at a frequency of 20 Hz and stored by means of the EDISOL software package  
23 (Moncrieff et al., 1997). The EdiRE software (version 1.4.3.1021, R. Clement, University of  
24 Edinburgh) was used to compute turbulent CO<sub>2</sub> fluxes from the raw data.

25 Along with EC flux measurements, the main meteorological and soil physical variables were  
26 measured. Among these: short and long-wave radiation components (Kipp & Zonen CNR1,  
27 Delft, The Netherlands), incoming total and diffuse PAR (LI-COR LI- 190SA, Lincoln, USA;  
28 and Delta-T BF3H, Cambridge, UK), precipitation (Young 52202H, Traverse City, Michigan,  
29 USA), air humidity and temperature (Rotronic MP103A, Crawley, UK), soil temperature  
30 profile at depths of 2, 5, 10, 20 and 50 cm (STP01, Hukseflux, Delft, The Netherlands), and  
31 volumetric soil water content at depths of 10 and 20 cm (CS615 reflectometers, Campbell

1 Scientific inc., Logan, Utah, USA). All meteorological variables were recorded at 1 min  
2 intervals and averaged over 30 minutes; both 1-min data and half-hourly averages were stored  
3 on a CR23X datalogger (Campbell Scientific Inc., Logan, Utah, USA).

4 Half-hourly measurements of net ecosystem exchange (NEE) were gap-filled and partitioned  
5 into ecosystem respiration (Reco) and gross ecosystem production (GEP) by means of the  
6 online tool developed by Reichstein et al. (2005) ([http://www.bgcjena.mpg.de/bgcmdi/html/  
7 eddyproc/](http://www.bgcjena.mpg.de/bgcmdi/html/eddyproc/)). However, only not gap-filled data were analyzed in this study.

8 To maintain consistency between the time-window used for calculating vegetation reflectance  
9 and narrow-band VIs, the mean midday gross ecosystem production ( $GEP_m$ ,  $\mu\text{mol m}^{-2} \text{s}^{-1}$ )  
10 and mean midday incoming photosynthetically active radiation ( $PAR_m$ ,  $\mu\text{mol m}^{-2} \text{s}^{-1}$ ) were  
11 calculated for the same time period used for vegetation spectral properties (11:00 a.m. - 1:00  
12 p.m. of local solar time).

13 Further details regarding the EC instrumentation, data elaboration and quality control can be  
14 found in Marcolla et al. (2011).

### 15 **2.3 Multispectral reflectance and narrow-band vegetation indices**

16 Multispectral data were acquired on a continuous basis from 2008 to 2012 by means of the  
17 Cropscan Multispectral Radiometer system MSR16R (Cropscan Inc., Rochester, USA). The  
18 system consists of a 16-band radiometer (simultaneously measuring reflected and incoming  
19 radiation in narrow spectral bands) and a datalogger controller (DLC) storing the acquired  
20 data (Table 1). For each band, the incoming solar irradiance is measured through a cosine  
21 diffuser, while reflected radiance is measured through a  $28^\circ$  field of view foreoptic. The  
22 system was installed on the existing EC tower at a height of 6 m, which allowed the  
23 observation of a 3.0 m diameter vegetation surface. The instrument was operated during 5  
24 growing seasons (15/05-21/11/2008, 20/05-1/11/2009, 19/05-24/10/2010, 11/05-3/09/2011  
25 and 18/05-30/09/2012), for a total of 758 days.

26 Before the beginning of each growing season, the system was calibrated using the method  
27 recommended by the manufacturer, based on the use of a white reference panel with known  
28 reflectance (<http://www.cropscan.com/wsupdn.html>). Additionally, CROPSCAN, Inc.  
29 provided cosine response calibration data with each upward facing MSR16 module and  
30 temperature sensitivity calibration data. Both cosine and temperature corrections were

1 included in the postprocessing software (POSTPROC program) provided with the MSR  
2 system.

3 Incident irradiance and reflected radiance were collected every 10 min and reflectance at  
4 given wavelengths was calculated. In order to minimize solar angle effects, reflectance data  
5 were finally averaged over two hours close to a solar noon (11:00 a.m. - 1:00 p.m. of local  
6 solar time).

7 Due to the noisy and unreliable optical signal beyond 1000 nm (bands nr 15 and 16; Table 1),  
8 only the data of the first 14 bands were included in the analyses. In addition, data were  
9 excluded when: 1) the site was covered by snow, 2) precipitation was recorded 2 hours prior  
10 or during the midday averaging period, and 3) the weather conditions did not allow for the  
11 removal of the cut biomass from the footprint of CropsScan system (and EC tower) straight  
12 after the cut event. According to these quality criteria, 24% of the data were discarded, mainly  
13 due to the meteorological conditions.

14 Canopy reflectance spectra were then used for computing the VIs. Although many different  
15 VIs were investigated (Table A1), only the most commonly used and the best performing in  
16  $GEP_m$  estimation - considering all the 5 years of observations - are presented in the study. The  
17 list of the five presented VIs is reported in Table 2.

## 18 **2.4 Models for $GEP_m$ estimation**

19 In order to estimate  $GEP_m$  we used two approaches, one based on linear regression (using the  
20 concept of the LUE model) and the other on multiple regression. The first approach assumed  
21 a direct linear relationship between  $GEP_m$  and VIs (model 1) and between  $GEP_m$  and the  
22 product of VIs and  $PAR_m$  (model 2). In the second approach, the interaction effects between  
23 different variables were explored by running two stepwise bidirectional multiple regression  
24 models, in which  $GEP_m$  was set as a dependent variable and reflectance (model 3), or  
25 reflectance and  $PAR_m$  (model 4), as explanatory variables. The above mentioned models  
26 (Table 3) were tested both for each year on a separate basis, and for all the years together in  
27 order to obtain the general models for the estimation of  $GEP_m$ .

## 28 **2.5 Statistical analysis**

29 Pearson's correlation analysis was used to test the significance of the relationships between  
30  $GEP_m$  and VIs or  $VIs*PAR_m$ .

1 In order to evaluate how robust the relationships between  $GEP_m$  and VIs were, the slopes of  
2 the linear regressions between the best performing VI against  $GEP_m$  were analyzed. In  
3 particular, the slopes of the regressions obtained for each year and obtained in the general  
4 model 1 (including all 5 years) were compared by means of a t-test to check whether the  
5 regression coefficients were statistically different.

6 Besides, a multiple stepwise bidirectional linear regression was used to explore the interaction  
7 effects between variables (considering  $GEP_m$  as a dependent variable and reflectance at  
8 fourteen analyzed wavelengths (model 3), or reflectance values and  $PAR_m$  (model 4), as  
9 explanatory variables) to find the model that best fits the data according to the Akaike's  
10 information criterion (AIC; Akaike, 1973). The variance inflation factor (VIF; Mason et al.,  
11 2003) was used to measure the degree of (multi)collinearity of the  $i$ th independent variable  
12 with the other independent variables in the regression models.

13 When VIF for any of the predictors reached the threshold value of 10, the (multi)collinearity  
14 was reduced by eliminating one independent variable (the last one selected by the automatic  
15 stepwise bidirectional regression) from the analysis (O'Brien, 2007). The procedure was  
16 repeated until none of the VIF factors exceeded the acceptable threshold value, thus the subset  
17 of explanatory variables was free of significant (multi)collinearity issues.

18 The final subset of the predictor variables was selected by testing whether the increase of the  
19 adjusted  $R^2$  ( $adjR^2$ ) after adding a subsequent predictor variable to the multiple regression  
20 model was significantly different from zero (at significance level  $\alpha=0.001$ ). Multiple  
21 regression models were compared by means of the Fisher test.

22 Each of the four model's coefficients was obtained by fitting each model against  $GEP_m$ . The  
23 main goodness of fit statistics (adjusted coefficient of determination –  $adjR^2$ , root mean square  
24 error – RMSE, percentage root mean square error – PRMSE and probability value –  $p$ ) were  
25 computed to compare the performance of the different models.

26 Additionally, a validation of the best performing general models using training/validation  
27 splitting approach, in which one year at a time was excluded from the dataset, was conducted.  
28 The remaining 4 years subset was used as a training set and the excluded year as a validation  
29 set. The model was fitted (calibrated) against each training set and the resulting  
30 parameterization was used to predict the  $GEP_m$  of the excluded year. Validation accuracy was  
31 evaluated in terms of RMSE.



1 All the statistical analyses were performed by means of the R software (version 2.15.2,  
2 <http://www.r-project.org/>).

### 3 **2.6 The gap scenarios**

4 In order to evaluate the ability of spectral models to gap-fill CO<sub>2</sub> flux data, secondary datasets  
5 were generated by flagging ~16 % of the 5 growing seasons data as unavailable (artificial  
6 gaps constituting 90 observation days out of 573 available observation days). The percentage  
7 of artificial gaps was chosen due to the fact that during the observation period of the study (~  
8 May to November, 2008-2012) the EC dataset had an average of 16 % of missing or rejected  
9 values of NEE data collected during midday hours. Following Moffat et al. (2007) these  
10 artificial gaps were superimposed on the already incomplete data, without regard for the  
11 distribution of real gaps in the time series. Three gap length scenarios were considered: gaps  
12 of 1, 3 and 5 observation days. The artificial gaps were distributed randomly and each of the  
13 three scenarios was permuted 10 times and results were averaged (Moffat et al., 2007).  
14 Secondary datasets with artificial gaps were used to calibrate the models that were applied for  
15 filling GEP<sub>m</sub> data. The gap-filling statistical metrics ( $\text{adj}R^2$ , RMSE, PRMSE) were calculated  
16 using the EC derived GEP<sub>m</sub> in these artificial gaps to validate the predictions of filling  
17 technique.

18

### 19 **3 Results**

20 Figure 1 shows the seasonal variations of (a) PAR<sub>m</sub> and (b) GEP<sub>m</sub>. During the snow-free  
21 period (May-November) the average PAR<sub>m</sub> was 1073 ( $\pm 472$ ), 1167 ( $\pm 485$ ), 1068 ( $\pm 581$ ),  
22 1199 ( $\pm 463$ ) and 1065 ( $\pm 523$ )  $\mu\text{mol m}^{-2} \text{s}^{-1}$  in 2008, 2009, 2010, 2011 and 2012, respectively,  
23 with maximum values of approximately 2000  $\mu\text{mol m}^{-2} \text{s}^{-1}$ . The maximum difference in  
24 PAR<sub>m</sub> means among the investigated growing seasons was less than 11.5 %. Mean daily air  
25 temperature (Fig. 2) for the same period was 9.1 ( $\pm 5.3$ ), 10.0 ( $\pm 5.2$ ), 8.4 ( $\pm 5.6$ ), 9.8 ( $\pm 4.8$ ) and  
26 10.0 ( $\pm 5.3$ ) °C in 2008, 2009, 2010, 2011 and 2012, respectively, and the maximum  
27 difference between temperature means was equal to 15.6 %. A higher variability was  
28 observed in total precipitation recorded from May to November (Fig. 2). The differences in  
29 precipitation sums between the investigated years reached up to 50 %. The precipitation  
30 amount in 2011 (1008 mm) was similar to the 20 year period average (990 mm, 1993-2012).  
31 The growing season of 2010 (1473 mm) was particularly wet, with a precipitation sum 49%

1 higher than the long term average, while 2009 (744 mm) was fairly dry, with a total  
2 precipitation 25 % lower than the average sum of precipitation in 1993-2012. The  
3 precipitation amounts in 2008 (1193 mm) and 2012 (1305 mm) were higher than the 20 year  
4 period average by 21 % and 32 %, respectively.

5 Seasonal patterns of  $GEP_m$  were driven by both, environmental variables (such as incoming  
6 PAR and air temperature) and grassland management (Marcolla et al., 2011). The grassland  
7 cut occurred around mid-July, and split the growing season into two sub-periods. The  
8 maximum gross  $CO_2$  flux rates were recorded in the early summer (end of June - mid July).  
9 After the cut event, the canopy regrowth generally reached a peak at the beginning of  
10 September.

11 The VIs showed a similar behavior to  $GEP_m$  and the peaks of these time series were almost  
12 synchronous. Starting from the early part of September VIs began decreasing gradually in all  
13 the investigated years due to the senescence phase (characterized by a progressive canopy  
14 yellowing and wilting), but at varied rates.

15 Examples of seasonal courses of investigated VIs and  $GEP_m$  measured in 2012 are shown in  
16 Fig. 3. For better visualization and easier comparison, both  $GEP_m$  and VIs were normalized  
17 by scaling between 0 and 1. The graphs which refer to other years of observations can be  
18 found in Fig. B1.

19 The linear regression analysis (Table 4) showed that the presented VIs explained at least 50%  
20 of the variability of  $GEP_m$ .

21 The highest accuracy of model 1 was obtained in 2009 and 2012 ( $adjR^2$  up to 0.81). On the  
22 other hand, the lowest accuracy of the same model was reported in 2011 ( $max adjR^2=0.64$ ).  
23 This low value of  $adjR^2$  could be explained by the fact that during this year the CropScan  
24 sensor was not operated during the autumn period, and thus the range of VIs and  $GEP_m$  was  
25 smaller as the senescence phase was missed (Table 4).

26 The estimation accuracy was also dependent on the VIs used for the parameterization of  
27 model 1 (Table 4). VIs, including the red-edge band in their formulation, turned out to be the  
28 best candidates for  $GEP_m$  estimations considering both the general model and the five  
29 different years on a separate basis. The MSR, although it is based on the NIR and red bands,  
30 also showed reliable performance. Taking into account the models for the single years MSR,  
31 DR, and  $CI_{red-edge}$  were included in the group of the three best fitting models 3, 2 and 4 times,

1 respectively.  $NDVI_{red-edge}$  was in the group of the three best performing models in each  
2 investigated year. In contrary, NDVI was never included among the best predictors of  $GEP_m$   
3 (Table 4).

4 The best estimation accuracy obtained when model 1 was parameterized with  $NDVI_{red-edge}$   
5 resulted in PRMSE of 21.14 %, 14.49 %, 17.20 %, 13.80 % and 11.29 % for 2008, 2009,  
6 2010, 2011 and 2012, respectively. The comparison of linear regression slopes between  
7  $NDVI_{red-edge}$  against  $GEP_m$  between each single year and the general model (which considered  
8 all 5 years of observation together) (Fig. 4), showed that only the slopes of these linear  
9 relationships in 2011 and 2012 were significantly different from the general model ( $p=0.02$   
10 and 0.01 for 2011 and 2012, respectively). The other years (2008, 2009, 2010) were  
11 statistically indistinguishable from the general model (slopes:  $p>0.90$ ,  $p>0.46$ ,  $p>0.89$  for  
12 2008, 2009, 2010, respectively). This contributed to the fact that  $NDVI_{red-edge}$  explained more  
13 than 74% of the variability of  $GEP_m$  during the 5 years of observations (PRMSE of 16.40 %)  
14 (Table 4).

15 The inclusion of incoming  $PAR_m$  into the model resulted in a general decrease of its  
16 performance. The PRMSE was on average 14.64 % higher in model 2 than in model 1  
17 considering all of the 5 years of observations. As an example, the  $adjR^2$  of the general model  
18 (2008-2012) fed with  $NDVI_{red-edge}$  decreased from 0.74 to 0.61, RMSE increased from 3.41 to  
19  $4.19 \mu mol m^{-2} s^{-1}$  and PRMSE increased from 16.40 to 20.18 %. A similar pattern was  
20 observed in each of the investigated years (Table 4).

21 In order to investigate the impact of radiation quality on these results, the light response of  
22 half-hourly GEP (data collected between 11:00 a.m. and 1:00 p.m; during the snow-free  
23 period of 2012) considering different levels of diffuse radiation was investigated. Two  
24 different relationships between GEP and incoming PAR were found: one for cloudy  
25 conditions (when diffusion index - DI, which is the ratio between diffuse and total incident  
26 PAR, exceeded 0.7) and one for sunny conditions ( $DI<0.3$ ) (Fig. 5). The data when the above  
27 mentioned populations were overlapping (PAR from 800 to  $1350 \mu mol m^{-2} s^{-1}$ ) indicated that,  
28 in the Monte Bondone grassland site, photosynthesis rates were significantly higher under  
29 diffuse compared to direct radiation.

30 A stepwise bidirectional procedure selected reflectance (R) at 681, 781 and 720 nm (model 3)  
31 and R681, R781,  $PAR_m$  and R720 (model 4) as significant drivers of  $GEP_m$ , considering each  
32 of the 5 years of observations simultaneously (Table 5).

1 It is interesting to note that in model 3, referring to each observation year on a separate basis  
2 (data not shown), the red-edge bands were included as important predictors in all of the five  
3 investigated years. The red region was chosen as a highly predictive variable in 40% of cases,  
4 while the NIR region in three out of five investigated growing seasons. In model 4, red and  
5 NIR bands contributed to the stepwise regression model in three and two out of five  
6 observation years, respectively.  $PAR_m$ , as an additional variable of model 4, was included in  
7 the model three out of five times. The range of  $adjR^2$  values for different years considered on  
8 a separate basis varied from 0.61 to 0.87 and from 0.70 to 0.88 for model 3 and 4,  
9 respectively (data not shown).

10 A stepwise bidirectional multiple regression with reflectance at 681, 781 and 720 nm as  
11 predictors did not yield any improvement in the explained variance of  $GEP_m$  when the entire  
12 dataset was considered ( $adjR^2=0.74$  - general model 1;  $adjR^2=0.73$  - general model 3; Table 4  
13 and 5, respectively). Also, adding  $PAR_m$  as an independent variable of the model resulted  
14 only in a slight improvement in the accuracy of the  $GEP_m$  estimation compared to the general  
15 linear regression model 1 based on  $NDVI_{red-edge}$ . In fact, the  $adjR^2$  increased from 0.74 to 0.79,  
16 while the PRMSE decreased from 16.40 to 14.75 % (Table 4 and 5).

17 Validation of model 1 based on  $NDVI_{red-edge}$  showed that there was no relevant difference in  
18 prediction accuracy among validation years (RMSE was varying between 3.12 and 3.85  $\mu\text{mol}$   
19  $\text{m}^{-2} \text{s}^{-1}$ , Figure 6). Validation results of general model 4 showed that considering all the 5  
20 validated years RMSE was on average 3.26  $\mu\text{mol} \text{m}^{-2} \text{s}^{-1}$ .

21 The differences in the  $adjR^2$  performance of the gap-filling scenarios showed that the accuracy  
22 of gap filling decreased slightly with gap length, while the range of the goodness of fit  
23 statistics ( $adjR^2$ , RMSE, PRMSE) generally increased with gap size (Table 6). However, on  
24 average,  $GEP_m$  gaps were filled with an accuracy of 73% with model 1 fed with  $NDVI_{red-edge}$   
25 (RMSE=3.40  $\mu\text{mol} \text{m}^{-2} \text{s}^{-1}$ , PRMSE= 16.48 %), and with an accuracy of 76% (RMSE=3.14  
26  $\mu\text{mol} \text{m}^{-2} \text{s}^{-1}$ , PRMSE= 15.25 %) with model 4 using reflectance at 681, 720 and 781 nm and  
27  $PAR_m$  data.

28

## 29 **4 Discussion**

30 Continuous and simultaneous measurements of narrow-band canopy reflectance and EC  
31 carbon dioxide fluxes have been successfully performed for five consecutive years in a

1 subalpine grassland ecosystem. The multispectral Cropscan MSR16R system demonstrated to  
2 be a reliable instrument for monitoring carbon fluxes. The results of this study provided  
3 important information on how consistent and robust the relationships between VIs and  $GEP_m$   
4 are in such a dynamic ecosystem. Additionally, they allowed the comparison of different  
5 approaches (correlation analysis and multiple regression) for predicting  $GEP_m$ .

6 Although several studies have already compared VIs obtained from in-situ observations  
7 against EC CO<sub>2</sub> fluxes (Gitelson et al., 2003b; Inoue et al., 2008; Peng and Gitelson, 2012;  
8 Peng et al., 2011; Rossini et al., 2010; Sims et al., 2006), and a few studies have focused on  
9 very similar canopies (Gianelle et al., 2009; Rossini et al., 2012; Wohlfahrt et al., 2010), we  
10 are not aware of any study based on such a long time series, acquired on a continuous basis  
11 during the growing seasons.

12 From the data presented, it follows that MSR and DR indices which are modified and  
13 improved variants of the most commonly used VIs showed generally slightly stronger linear  
14 relationship with  $GEP_m$  when compared to NDVI. Nevertheless, considering all of the  
15 observation years, the most robust estimates of  $GEP_m$  were obtained when  $NDVI_{red-edge}$  and  
16  $CI_{red-edge}$  were used to parameterize the model (Table 4). These results confirmed the findings  
17 of previous studies on both similar (Rossini et al., 2012) and different ecosystems (Gitelson et  
18 al., 2003b; Peng and Gitelson, 2012; Peng et al., 2011; Rossini et al., 2010), indicating that  
19 VIs based on the red-edge part of the spectrum are the most sensitive to the seasonal GEP  
20 dynamics due to their better linearity with chlorophyll content (Gitelson et al., 2003a; Sims  
21 and Gamon, 2002; Wu et al., 2008), and with green leaf area index - green LAI (Gitelson et  
22 al., 2003c; Viña et al., 2011). In general, VIs (such as NDVI) calculated as a normalized  
23 difference between NIR bands - characterized by a high reflectance due to leaf and canopy  
24 scattering, and visible bands (e.g. red), where absorption by the chlorophyll pigments is  
25 predominant (Jackson and Huete, 1991), tend to lose their sensitivity to moderate-high  
26 aboveground biomass due to the saturation of reflectance in the visible bands and due to the  
27 limitation of the normalized difference approach (Fava et al., 2007; Gao et al., 2000; Mutanga  
28 and Skidmore, 2004). Better performances of  $NDVI_{red-edge}$  and  $CI_{red-edge}$  stem from the fact  
29 that even though the red-edge part of the spectrum is characterized by lower absorption by  
30 chlorophyll, it still remains sensitive to changes in its content, reducing the saturation effect  
31 and enhancing the sensitivity of these VIs to moderate-high vegetation densities (Clevers and  
32 Gitelson, 2013; Wu et al., 2008).

1 Incorporating  $PAR_m$  into the model resulted in a general decrease in the goodness of fit of the  
2 linear regression. One reason for this is that sunlight is used by plants more efficiently under  
3 cloudy than clear sky conditions due to a more uniform illumination of the canopy, and thus a  
4 smaller fraction of the canopy likely to be light saturated (Baldocchi and Amthor, 2001; Chen  
5 et al., 2009; Mercado et al., 2009). Accordingly, significantly higher photosynthesis rates  
6 under diffuse as regards to direct radiation conditions (with similar values of PAR) were  
7 noted in the Monte Bondone site (Fig. 5). Similar results have been reported by Rossini et al.  
8 (2012), who also pointed out that, in a similar subalpine grassland ecosystem, the inclusion of  
9 incident PAR in a model formulation did not result in an improved estimation of GEP.  
10 However, in several other studies referring to other dynamic ecosystems, GEP was  
11 successfully estimated as a product of VIs and PAR (Peng and Gitelson, 2012; Rossini et al.,  
12 2010; Wu et al., 2009). A recent study of Peng et al. (2013) confirmed that the use of PAR in  
13 the model can introduce noise and unpredictable uncertainties in GEP estimations. As  
14 suggested by these authors, the response of productivity to changes in PAR is quite complex  
15 and is influenced by many variables such as vegetation physiological status, canopy structure  
16 and light distribution in the canopy. Some other authors also brought to light some important  
17 aspects related to the use of PAR. Sims et al. (2008) showed that the variation in PAR is a  
18 more relevant determinant of GEP over very short timescales, and appears to be important for  
19 diurnal trends. Gitelson et al. (2012) demonstrated that seasonal variation of PAR potential  
20 (defined as the maximal value of incident PAR that may occur when the concentrations of  
21 atmospheric gasses and aerosols are minimal) can be used to improve the performance of the  
22 models. Therefore, further analyses of the response of different vegetation types to various  
23 levels of diffuse radiation are required, and the hypothesis that the DI and PAR potential can  
24 improve the performance of the models including radiation as an input parameter needs to be  
25 verified.

26 The use of the reflectance approach instead of the VIs approach did not lead to considerably  
27 improved results in estimating  $GEP_m$ . Including additional predictors in multiple stepwise  
28 regression resulted in only a 6% improvement of the explained variance, considering all of the  
29 5 years of observations collectively. We believe this was partly due to the limited number of  
30 available bands of the CropScan system, and that further studies are needed to explore the  
31 benefits of using hyperspectral data for predicting  $CO_2$  uptake across different terrestrial  
32 ecosystems types.

1 A detailed analysis of the full vegetation spectrum and of the various spectral absorption  
2 features appears to be particularly meaningful for providing a solid basis for up-scaling of  
3 GEP estimations using airborne and satellite platforms.

4 In this study the reflectance value at 720 nm, which was used in the multiple regression  
5 models, did not bring a relevant increase in the  $\text{adj}R^2$  values (partial  $\text{adj}R^2$  was 0.04 and 0.03  
6 for model 3 and 4, respectively). On the other hand, the successful performance of VIs using  
7 this band confirms the important role of this part of the spectrum in monitoring the dynamics  
8 of ecosystem carbon dioxide fluxes.

9 Validation results of general model 1 fed with  $\text{NDVI}_{\text{red-edge}}$  showed that RMSE increased on  
10 average from 3.41 to 3.48  $\mu\text{mol m}^{-2} \text{s}^{-1}$ , compared to non-validated general model 1  
11 (averaging the values obtained from the 5 different validation years). Validation results of  
12 general model 4 showed that RMSE increased on average from 3.06 to 3.26  $\mu\text{mol m}^{-2} \text{s}^{-1}$ ,  
13 compared to non-validated general model 4. The highest decrease of the  $\text{GEP}_m$  estimation  
14 accuracy was noted in the growing season of 2012 (Table 4, Figure 6), which was presumably  
15 caused by the unusual drought which occurred just after the cut event. The precipitation to  
16 temperature ratio for a 15 day period after the cut in the growing season of 2012 was more  
17 than 10 times lower than in the other years and this fact could have affected  $\text{GEP}_m$  to a higher  
18 extent than VIs related to canopy “greenness”. As a consequence, models calibrated with the  
19 first four years of the dataset overestimated the  $\text{GEP}_m$  measured in the second part of the  
20 growing season of 2012.

21 During the observation period, the study site experienced a high variability in both  
22 precipitation and air temperature (covering approximately 88% and 54% of the variability  
23 observed in a 20 year period for precipitation and temperature, respectively) (Fig 2). General  
24 model 1 parameterized with  $\text{NDVI}_{\text{red-edge}}$  ( $\text{adj}R^2=0.74$ ), and general model 3 ( $\text{adj}R^2=0.73$ ) and  
25 4 ( $\text{adj}R^2=0.79$ ) based on the reflectance data were successful in capturing the inter-annual  
26 variability of  $\text{GEP}_m$  among the 5 years characterized by different climatic conditions.  
27 Therefore, these results support the use of ground spectral measurements for monitoring  
28  $\text{GEP}_m$  in a long-term framework. We must however emphasize that the possible limitation of  
29 the approach based on VIs related to “canopy greenness” is that variations of GEP due to the  
30 short term environmental stresses cannot be monitored by these VIs, unless these stresses  
31 affect chlorophyll content (Gitelson et al., 2008).

1 Combining proximal sensing with EC observations may be relevant also for the EC data gap-  
2 filling. In fact, the accuracy and reliability of the EC measurements depend on certain  
3 theoretical assumptions (e.g. requirement for: turbulent and non-advective atmospheric  
4 conditions, stationarity of the measured fluxes) which often cannot be fulfilled in real field  
5 conditions (Foken et al., 2004; Göckede et al., 2004; Papale et al., 2006). The need of  
6 rejecting data acquired during periods when the above-mentioned micrometeorological  
7 conditions were not met or due to other reasons such as non-optimal wind directions,  
8 equipment failures etc. results in dataset gaps constituting from 20% to 60% of annual data  
9 (Falge et al., 2001; Hui et al., 2004; Moffat et al., 2007). One of the most widely used gap-  
10 filling routines is based on the modeling of flux data with available environmental variables  
11 by means of nonlinear regression (Aubinet et al., 2000; Falge et al., 2001). This technique  
12 uses two equations, one for the response of ecosystem respiration ( $R_{eco}$ ) to temperature and  
13 one for the light response of GEP (Moffat et al., 2007), allowing their predictions during gaps.  
14 The implementation of VIs into the light response model might help to improve the gap filling  
15 results, especially in very dynamic ecosystems such as croplands, grasslands or deciduous  
16 forests. This could be particularly useful in case of long gaps in the EC data, which are  
17 inherently associated with a large degree of uncertainty (Moffat et al., 2007; Richardson and  
18 Hollinger, 2007; Wohlfahrt et al., 2010) and in case of managed ecosystems, where carbon  
19 dioxide uptake depends not only on the incoming radiation seasonality, but also on cutting  
20 and grazing events. The results of a simple gap filling approach presented in this study (based  
21 on creating and superimposing randomly distributed artificial gaps of three different lengths  
22 on the real dataset and comparing  $GEP_m$  values derived from EC with  $GEP_m$  values filled with  
23 the best performing spectral models) encourage the use of spectral data in the gap filling  
24 procedures of EC flux time series. The spectral based models were able to predict  $GEP_m$   
25 values with a performance comparable with others methods (Moffat et al., 2007) with  $adjR^2$   
26 ranging from 0.70 (5 days long gap, general model 1 parameterized with  $NDVI_{red-edge}$ ) to 0.78  
27 (1 day long gap, general model 4 based on reflectance at 681, 720 and 781 nm and  $PAR_m$   
28 data) (Table 6).

29

## 30 **5 Conclusions**

31 This study investigated the potential of a commercially available system - based on a 16 band  
32 multispectral sensor - for monitoring mean midday gross ecosystem production ( $GEP_m$ ) in a



1 dynamic subalpine grassland ecosystem of the Italian Alps. Chlorophyll-related indices  
2 including the red-edge part of the spectrum in their formulation (such as  $\text{NDVI}_{\text{red-edge}}$  and  
3  $\text{CI}_{\text{red-edge}}$ ) were the best predictors of  $\text{GEP}_m$ , and were able to explain most of its variability  
4 ( $\text{adj}R^2 = 0.74$  for  $\text{NDVI}_{\text{red-edge}}$ ,  $\text{adj}R^2 = 0.73$  for  $\text{CI}_{\text{red-edge}}$ ) during the five consecutive years of  
5 observations, characterized by different climatic conditions. Our results confirm the findings  
6 of the literature regarding the complexity of the response of ecosystem productivity to change  
7 in PAR (Peng et al., 2013). This response is influenced by many variables and in fact, in our  
8 study, the accuracy of  $\text{GEP}_m$  estimation decreased after including incident  $\text{PAR}_m$  into the  
9 linear regression model and the photosynthesis process was shown to be more efficient under  
10 diffuse compared to direct radiation. Further investigations are planned in order to explore the  
11 utility of including DI and PAR potential in the models to improve their performances. Also,  
12 the use of the reflectance approach instead of the VIs approach did not lead to considerably  
13 improved results in estimating  $\text{GEP}_m$ . Although a more detailed analysis of the full vegetation  
14 spectrum is desirable (for providing best performing algorithms and a solid basis for in-situ  
15 validation and up-scaling of optical models to the airborne and satellite platforms), the results  
16 indicate that such relatively low-cost multispectral sensors can be adopted to provide a  
17 significant contribution in monitoring carbon dioxide fluxes and biophysical parameters in  
18 dynamic ecosystems, for improving gap-filling techniques and for further integration into  
19 more complex biogeochemical models.

20

## 21 **Acknowledgements**

22 The authors would like to acknowledge Maurizio Bagnara, PhD student of Fondazione  
23 Edmund Mach, for help in R programming and John Gamon, Profesor from University of  
24 Alberta, for fruitful discussions. The authors would like to thank the editor and the two  
25 reviewers (Anatoly Gitelson, and the anonymous reviewer) of this manuscript for their  
26 valuable comments which have helped to improve the overall quality of the paper.

## 1 **References**

- 2 Akaike, H.: Information theory and an extension of the maximum likelihood principle, in:  
3 Proceedings of the Second International Symposium on Information Theory, edited by:  
4 Petrov, B. N. and Csaki, F., Akademiai Kiado, Budapest, 267–281 (Reproduced in:  
5 Breakthroughs in Statistics, edited by: Kotz, S. and Johnson, N. L., 2003), Vol. I, Foundations  
6 and Basic Theory, Springer-Verlag, New York, 610–624, 1973.
- 7 Aubinet, M., Grelle, A., Ibrom, A., Rannik, Ü., Moncrieff, J., Foken, T., Kowalski, A. S.,  
8 Martin, P. H., Berbigier, P., Bernhofer, C., Clement, R., Elbers, J., Granier, A., Grünwald, T.,  
9 Morgenstern, K., Pilegaard, K., Rebmann, C., Snijders, W., Valentini, R., and Vesala, T.:  
10 Estimates of the Annual Net Carbon and Water Exchange of Forests: The EUROFLUX  
11 Methodology, *Adv. Ecol. Res.*, 30, 113–175, 2000.
- 12 Baldocchi, D. D.: Assessing the eddy covariance technique for evaluating carbon dioxide  
13 exchange rates of ecosystems: past, present and future, *Glob. Chang. Biol.*, 9, 479–492, 2003.
- 14 Baldocchi, D. D. and Amthor, J. S.: Canopy Photosynthesis: History , Measurements, and  
15 Models, in: *Terrestrial Global Productivity: Past, Present and Future*, edited by J. Roy, B.  
16 Saugier, and H. Mooney, Academic Press, San Diego, 9–31, 2001.
- 17 Balzarolo, M., Anderson, K., Nichol, C., Rossini, M., Vescovo, L., Arriga, N., Wohlfahrt, G.,  
18 Calvet, J.-C., Carrara, A., Cerasoli, S., Cogliati, S., Daumard, F., Eklundh, L., Elbers, J. A.,  
19 Evrendilek, F., Handcock, R. N., Kaduk, J., Klumpp, K., Longdoz, B., Matteucci, G., Meroni,  
20 M., Montagnani, L., Ourcival, J.-M., Sánchez-Cañete, E. P., Pontailler, J.-Y., Juszczak, R.,  
21 Scholes, B., and Martín, M. P.: Ground-Based Optical Measurements at European Flux Sites:  
22 A Review of Methods, Instruments and Current Controversies, *Sensors*, 11, 7954–7981,  
23 doi:10.3390/s110807954, 2011.
- 24 Blackburn, G. A.: Spectral indices for estimating photosynthetic pigment concentrations: a  
25 test using senescent tree leaves, *Int. J. Remote Sens.*, 19(4), 657–675,  
26 doi:10.1080/014311698215919, 1998.
- 27 Burba, G.: Eddy Covariance Method for Scientific, Industrial, Agricultural, and Regulatory  
28 Applications: A Field Book on Measuring Ecosystem Gas Exchange and Areal Emission  
29 Rates, LI-COR Biosciences, Lincoln, NE, USA., 2013.
- 30 Canadell, J. G., Mooney, H. A., Baldocchi, D. D., Berry, J. A., Ehleringer, J. R., Field, C. B.,  
31 Gower, S. T., Hollinger, D. Y., Hunt, J. E., Jackson, R. B., Running, S. W., Shaver, G. R.,

1 Steffen, W., Trumbore, S. E., Valentini, R., and Bond, B. Y.: Commentary: Carbon  
2 Metabolism of the Terrestrial Biosphere: A Multitechnique Approach for Improved  
3 Understanding, *Ecosystems*, 3, 115–130, doi:10.1007/s100210000014, 2000.

4 Carlson, T. N. and Ripley, D. A.: On the Relation between NDVI , Fractional Vegetation  
5 Cover , and Leaf Area Index, *Remote Sens. Environ.*, 62, 241–252, 1997.

6 Chen, J., Shen, M., and Kato, T.: Diurnal and seasonal variations in light-use efficiency in an  
7 alpine meadow ecosystem: causes and implications for remote sensing, *J. Plant Ecol.*, 2(4),  
8 173–185, doi:10.1093/jpe/rtp020, 2009.

9 Clevers, J. G. P. W. and Gitelson, A. A.: Remote estimation of crop and grass chlorophyll and  
10 nitrogen content using red-edge bands on Sentinel-2 and -3, *Int. J. Appl. Earth Obs. Geoinf.*,  
11 23, 344–351, doi:10.1016/j.jag.2012.10.008, 2013.

12 Dash, J. and Curran, P. J.: The MERIS terrestrial chlorophyll index, *Int. J. Remote Sens.*,  
13 25(23), 5403–5413, doi:10.1080/0143116042000274015, 2004.

14 Datt, B.: A New Reflectance Index for Remote Sensing of Chlorophyll Content in Higher  
15 Plants: Tests using Eucalyptus Leaves, *J. Plant Physiol.*, 154, 30–36, doi:10.1016/S0176-  
16 1617(99)80314-9, 1999.

17 Daughtry, C. S. T., Walthall, C. L., Kim, M. S., Brown de Colstoun, E., and McMurtrey III, J.  
18 E.: Estimating corn leaf chlorophyll concentration from leaf and canopy reflectance, *Remote*  
19 *Sens. Environ.*, 74, 229–239, 2000.

20 Falge, E., Baldocchi, D., Olson, R., Anthoni, P., Aubinet, M., Bernhofer, C., Burba, G.,  
21 Ceulemans, R., Clement, R., Dolman, H., Granier, A., Gross, P., Grünwald, T., Hollinger, D.,  
22 Jensen, N.-O., Katul, G., Keronen, P., Kowalski, A., Lai, C. T., Law, B. E., Meyers, T.,  
23 Moncrieff, J., Moors, E., Munger, J. W., Pilegaard, K., Rannik, Ü., Rebmann, C., Suyker, A.,  
24 Tenhunen, J., Tu, K., Verma, S., Vesala, T., Wilson, K., and Wofsy, S.: Gap filling strategies  
25 for defensible annual sums of net ecosystem exchange, *Agric. For. Meteorol.*, 107, 43–69,  
26 doi:10.1016/S0168-1923(00)00225-2, 2001.

27 Fava, F., Parolo, G., Colombo, R., Gusmeroli, F., Della Marianna, G., Monteiro, A.T., and  
28 Bocchi, S.: Fine-scale assessment of hay meadow productivity and plant diversity in the  
29 European Alps using field spectrometric data. *Agric. Ecosyst. Environ.*, 137, 151-157, 2010.

1 Foken, T., Göckede, M., Mauder, M., Mahrt, L., Amiro, B., and Munger, W.: Post-field Data  
2 Quality Control, in Handbook of Micrometeorology, pp. 181–208., 2004.

3 Gamon, J. A., Peñuelas, J., and Field, C. B.: A narrow-waveband spectral index that track  
4 diurnal changes in photosynthetic Efficiency, *Remote Sens. Environ.*, 41, 35–44, 1992.

5 Gamon, J. A., Rahman, A. F., Dungan, J. L., Schildhauer, M., and Huemmrich, K. F.:  
6 Spectral Network (SpecNet)-What is it and why do we need it?, *Remote Sens. Environ.*, 103,  
7 227–235, doi:10.1016/j.rse.2006.04.003, 2006.

8 Gamon J. A., Coburn, C., Flanagan, L., Huemmrich, K.F., Kiddle, C., Sanchez-Azofeifa, G.  
9 A., Thayer, D., Vescovo, L., Gianelle, D., Sims, D., Rahman, A. F., and Zonta Pastorella, G.:  
10 SpecNet revisited: bridging flux and remote sensing communities, *Can. J. Remote Sens.*,  
11 36(Suppl. 2), 376–390, doi:10.5589/m10-06, 2010.

12 Gao, X., Huete, A. R., Ni, W., and Miura, T.: Optical-Biophysical Relationships of  
13 Vegetation Spectra without Background Contamination, *Remote Seinsing Environ.*, 74, 609–  
14 620, 2000.

15 Geider, R. J., Delucia, E. H., Falkowski, P. G., Finzi, A. C., Grime, J. P., Grace, J., Kana, T.  
16 M., Roche, J. L. A., Long, S. P., Osborne, B. A., Platt, T., Prentice, I. C., Raven, J. A.,  
17 Schlesinger, W. H., Smetacek, V., Stuart, V., Sathyendranath, S., Thomas, R. B., Vogelmann,  
18 T. C., Williams, P., and Woodward, I. F.: Primary productivity of planet earth: biological  
19 determinants and physical constraints in terrestrial and aquatic habitats, *Glob. Chang. Biol.*, 7,  
20 849–882, 2001.

21 Gianelle, D. and Vescovo, L.: Determination of green herbage ratio in grasslands using  
22 spectral reflectance. Methods and ground measurements, *Int. J. Remote Sens.*, 28(5), 931–  
23 942, doi:10.1080/01431160500196398, 2007.

24 Gianelle, D., Vescovo, L., Marcolla, B., Manca, G. and Cescatti, A.: Ecosystem carbon fluxes  
25 and canopy spectral reflectance of a mountain meadow, *Int. J. Remote Sens.*, 30(2), 435–449,  
26 doi:10.1080/01431160802314855, 2009.

27 Gitelson, A. A.: Wide Dynamic Range Vegetation Index for remote quantification of  
28 biophysical characteristics of vegetation, *J. Plant Physiol.*, 161, 165–73, doi:10.1078/0176-  
29 1617-01176, 2004.

1 Gitelson, A. and Merzlyak, M. N.: Quantitative experiments estimation of chlorophyll-a using  
2 reflectance spectra: experiments with autumn chestnut and maple leaves, *J. Photochem.*  
3 *Photobiol.*, 22, 247–252, 1994.

4 Gitelson, A. A. and Merzlyak, M. N.: Remote estimation of chlorophyll content in higher  
5 plant leaves, *Int. J. Remote Sens.*, 18(12), 2691–2697, 1997.

6 Gitelson, A. A., Kaufman, Y. J., and Merzlyak, M. N.: Use of a Green Channel in Remote  
7 Sensing of Global Vegetation from EOS-MODIS, *Remote Sens. Environ.*, 58, 289–298, 1996.

8 Gitelson, A. A., Gritz, Y., and Merzlyak, M. N.: Relationships between leaf chlorophyll  
9 content and spectral reflectance and algorithms for non-destructive chlorophyll assessment in  
10 higher plant leaves, *J. Plant Physiol.*, 160, 271–82, doi:10.1078/0176-1617-00887, 2003a.

11 Gitelson, A. A., Verma, S. B., Viña, A., Rundquist, D. C., Keydan, G., Leavitt, B., Arkebauer,  
12 T. J., Burba, G. G., and Suyker, A. E.: Novel technique for remote estimation of CO<sub>2</sub> flux in  
13 maize, *Geophys. Res. Lett.*, 30(9), 1486, doi:10.1029/2002GL016543, 2003b.

14 Gitelson, A. A., Viña, A., Arkebauer, T. J., Rundquist, D. C., Keydan, G., and Leavitt, B.:  
15 Remote estimation of leaf area index and green leaf biomass in maize canopies, *Geophys.*  
16 *Res. Lett.*, 30(5), 1148, doi:10.1029/2002GL016450, 2003c.

17 Gitelson, A. A., Viña, A., Ciganda, V., Rundquist, D. C., and Arkebauer, T. J.: Remote  
18 estimation of canopy chlorophyll content in crops, *Geophys. Res. Lett.*, 32, L08403,  
19 doi:10.1029/2005GL022688, 2005.

20 Gitelson, A. A., Viña, A., Verma, S. B., Rundquist, D. C., Arkebauer, T. J., Keydan, G.,  
21 Leavitt, B., Ciganda, V., Burba, G. G., and Suyker, A. E.: Relationship between gross primary  
22 production and chlorophyll content in crops: Implications for the synoptic monitoring of  
23 vegetation productivity, *J. Geophys. Res.*, 111(D08S11), doi:10.1029/2005JD006017, 2006.

24 Gitelson, A. A., Viña, A., Masek, J. G., Verma, S. B. and Suyker, A. E.: Synoptic Monitoring  
25 of Gross Primary Productivity of Maize Using Landsat Data, *IEEE Geosci. Remote Sens.*  
26 *Lett.*, 5(2), 133–137, 2008.

27 Gitelson, A. A., Peng, Y., Masek, J. G., Rundquist, D. C., Verma, S., Suyker, A., Baker, J.  
28 M., Hatfield, J. L., and Meyers, T.: Remote estimation of crop gross primary production with  
29 Landsat data, *Remote Sens. Environ.*, 121, 404–414, doi:10.1016/j.rse.2012.02.017, 2012.

1 Glenn, E. P., Huete, A. R., Nagler, P. L., and Nelson, S. G.: Relationship between remotely-  
2 sensed vegetation indices, canopy attributes, and plant physiological processes: what  
3 vegetation indices can and cannot tell us about the landscape, *Sensors*, 8, 2136–2160, 2008.

4 Göckede, M., Rebmann, C., and Foken, T.: A combination of quality assessment tools for  
5 eddy covariance measurements with footprint modelling for the characterisation of complex  
6 sites, *Agric. For. Meteorol.*, 127, 175–188, doi:10.1016/j.agrformet.2004.07.012, 2004.

7 Haboudane, D., Miller, J. R., Pattey, E., Zarco-Tejada, P. J., and Strachan, I. B.:  
8 Hyperspectral vegetation indices and novel algorithms for predicting green LAI of crop  
9 canopies: Modeling and validation in the context of precision agriculture, *Remote Sens.*  
10 *Environ.*, 90, 337–352, doi:10.1016/j.rse.2003.12.013, 2004.

11 Harris, A. and Dash, J.: The potential of the MERIS Terrestrial Chlorophyll Index for carbon  
12 flux estimation, *Remote Sens. Environ.*, 114, 1856–1862, doi:10.1016/j.rse.2010.03.010,  
13 2010.

14 Huete, A., Didan, K., Miura, T., Rodriguez, E. P., Gao, X., and Ferreira, L. G.: Overview of  
15 the radiometric and biophysical performance of the MODIS vegetation indices, *Remote Sens.*  
16 *Environ.*, 83, 195–213, doi:10.1016/S0034-4257(02)00096-2, 2002.

17 Hui, D., Wan, S., Su, B., Katul, G., Monson, R., and Luo, Y.: Gap-filling missing data in eddy  
18 covariance measurements using multiple imputation (MI) for annual estimations, *Agric. For.*  
19 *Meteorol.*, 121, 93–111, doi:10.1016/S0168-1923(03)00158-8, 2004.

20 Inoue, Y., Peñuelas, J., Miyata, A., and Mano, M.: Normalized difference spectral indices for  
21 estimating photosynthetic efficiency and capacity at a canopy scale derived from  
22 hyperspectral and CO<sub>2</sub> flux measurements in rice, *Remote Sens. Environ.*, 112, 156–172,  
23 doi:10.1016/j.rse.2007.04.011, 2008.

24 Jackson, R. D. and Huete, A. R.: Interpreting vegetation indices, *Prev. Vet. Med.*, 11, 185–  
25 200, 1991.

26 Jordan, C.F.: Derivation of leaf area index from quality of light on the forest floor, *Ecology*,  
27 50, 663–666, 1969.

28 Kljun, N., Rotach, M. W., and Schmid, H. P.: A Three-Dimensional Backward Lagrangian  
29 Footprint Model For A Wide Range Of Boundary-Layer Stratifications, *Boundary-Layer*  
30 *Meteorol.*, 103, 205–226, 2001.

1 Lobell, D. B., Asner, G. P., Ortiz-Monasterio, J. I., and Benning, T. L.: Remote sensing of  
2 regional crop production in the Yaqui Valley, Mexico: estimates and uncertainties, *Agric.*  
3 *Ecosyst. Environ.*, 1944, 1–16, 2002.

4 Main, R., Cho, M. A., Mathieu, R., O’Kennedy, M. M., Ramoelo, A., and Koch, S.: An  
5 investigation into robust spectral indices for leaf chlorophyll estimation, *ISPRS J.*  
6 *Photogramm. Remote Sens.*, 66, 751–761, doi:10.1016/j.isprsjprs.2011.08.001, 2011.

7 Marcolla, B. and Cescatti, A.: Experimental analysis of flux footprint for varying stability  
8 conditions in an alpine meadow, *Agric. For. Meteorol.*, 135, 291–301,  
9 doi:10.1016/j.agrformet.2005.12.007, 2005.

10 Marcolla, B., Cescatti, A., Manca, G., Zorer, R., Cavagna, M., Fiora, A., Gianelle, D.,  
11 Rodeghiero, M., Sottocornola, M., and Zampedri, R.: Climatic controls and ecosystem  
12 responses drive the inter-annual variability of the net ecosystem exchange of an alpine  
13 meadow, *Agric. For. Meteorol.*, 151, 1233–1243, doi:10.1016/j.agrformet.2011.04.015, 2011.

14 Mason, R. L., Gunst, R. F., and Hess, J. L.: Variable Selection Techniques, in: *Statistical*  
15 *Design and Analysis of Experiments With Applications to Engineering and Science*, John  
16 Wiley & Sons, Hoboken, New Jersey, 672–674, 2003.

17 Mercado, L. M., Bellouin, N., Sitch, S., Boucher, O., Huntingford, C., Wild, M., and Cox, P.  
18 M.: Impact of changes in diffuse radiation on the global land carbon sink., *Nature*, 458, 1014–  
19 1017, doi:10.1038/nature07949, 2009.

20 Moffat, A. M., Papale, D., Reichstein, M., Hollinger, D. Y., Richardson, A. D., Barr, A. G.,  
21 Beckstein, C., Braswell, B. H., Churkina, G., Desai, A. R., Falge, E., Gove, J. H., Heimann,  
22 M., Hui, D., Jarvis, A. J., Kattge, J., Noormets, A., and Stauch, V. J.: Comprehensive  
23 comparison of gap-filling techniques for eddy covariance net carbon fluxes, *Agric. For.*  
24 *Meteorol.*, 147, 209–232, doi:10.1016/j.agrformet.2007.08.011, 2007.

25 Moncrieff, J. B., Massheder, J. M., de Bruin, H., Elbers, J., Friborg, T., Heusinkveld, B.,  
26 Kabat, P., Scott, S., Soegaard, H., and Verhoef, a.: A system to measure surface fluxes of  
27 momentum, sensible heat, water vapour and carbon dioxide, *J. Hydrol.*, 188-189, 589–611,  
28 doi:10.1016/S0022-1694(96)03194-0, 1997.

29 Monteith, J. L.: Solar Radiation and Productivity in Tropical Ecosystems, *J. Appl. Ecol.*, 9(3),  
30 747–766, 1972.

1 Monteith, J. L. and Moss, C. J.: Climate and the Efficiency of Crop Production in Britain,  
2 Philos. Trans. R. Soc. London B Biol. Sci., 281, 277–294, doi:10.1098/rstb.1977.0140, 1977.

3 Mutanga, O. and Skidmore, A.: Narrow band vegetation indices overcome the saturation  
4 problem in biomass estimation, *Int. J. Remote Sens.*, 25(19), 3999-4014, 2004.

5 Myneni, R. B. and Williams, D. L.: On the Relationship between FAPAR and NDVI, *Remote  
6 Sens. Environ.*, 49, 200–211, 1994.

7 O'Brien, R. M.: A Caution Regarding Rules of Thumb for Variance Inflation Factors, *Qual.  
8 Quant.*, 41, 673–690, doi:10.1007/s11135-006-9018-6, 2007.

9 Papale, D., Reichstein, M., Aubinet, M., Canfora, E., Bernhofer, C., Kutsch, W., Longdoz, B.,  
10 Rambal, S., Valentini, R., Vesala, T., and Yakir, D.: Towards a standardized processing of  
11 Net Ecosystem Exchange measured with eddy covariance technique: algorithms and  
12 uncertainty estimation, *Biogeosciences*, 3, 571–583, doi:10.5194/bg-3-571-2006, 2006.

13 Peng, Y. and Gitelson, A. A.: Remote estimation of gross primary productivity in soybean  
14 and maize based on total crop chlorophyll content, *Remote Sens. Environ.*, 117, 440–448,  
15 doi:10.1016/j.rse.2011.10.021, 2012.

16 Peng, Y., Gitelson, A. A., Keydan, G., Rundquist, D. C., and Moses, W.: Remote estimation  
17 of gross primary production in maize and support for a new paradigm based on total crop  
18 chlorophyll content, *Remote Sens. Environ.*, 115, 978–989, doi:10.1016/j.rse.2010.12.001,  
19 2011.

20 Peng, Y., Gitelson, A. A. and Sakamoto, T.: Remote estimation of gross primary productivity  
21 in crops using MODIS 250 m data, *Remote Sens. Environ.*, 128, 186–196, 2013.

22 Peñuelas, J., Gamon, J. A., Fredeen, A. L., Merino, J., and Field, C. B.: Reflectance indices  
23 associated with physiological changes in nitrogen and water-limited sunflower leaves,  
24 *Remote Sens. Environ.*, 48, 135–146, 1994.

25 Peñuelas, J., Baret, F., and Filella, I.: Semi-empirical indices to assess carotenoids/chlorophyll  
26 a ratio from leaf spectral reflectance, *Photosynthetica*, 31(2), 221–230, 1995.

27 Richardson, A. D. and Hollinger, D. Y.: A method to estimate the additional uncertainty in  
28 gap-filled NEE resulting from long gaps in the CO<sub>2</sub> flux record, *Agric. For. Meteorol.*, 147,  
29 199–208, doi:10.1016/j.agrformet.2007.06.004, 2007.



1 Rossini, M., Cogliati, S., Meroni, M., Migliavacca, M., Galvagno, M., Busetto, L.,  
2 Cremonese, E., Julitta, T., Siniscalco, C., Morra di Cella, U., and Colombo, R.: Remote  
3 sensing-based estimation of gross primary production in a subalpine grassland,  
4 *Biogeosciences*, 9, 2565–2584, doi:10.5194/bg-9-2565-2012, 2012.

5 Rossini, M., Meroni, M., Migliavacca, M., Manca, G., Cogliati, S., Busetto, L., Picchi, V.,  
6 Cescatti, A., Seufert, G., and Colombo, R.: High resolution field spectroscopy measurements  
7 for estimating gross ecosystem production in a rice field, *Agric. For. Meteorol.*, 150, 1283–  
8 1296, doi:10.1016/j.agrformet.2010.05.011, 2010.

9 Rouse, J.W., Haas, R. H., Schell, J. A., and Deering, D.W.: Monitoring Vegetation Systems in  
10 the Great Plains with ERTS, in: Third ERTS Symposium, NASA SP-353, Vol. 1, 309–317,  
11 US Government Printing Office, Washington, DC, 1974.

12 Running, S. W., Baldocchi, D. D., Turner, D. P., Gower, S. T., Bakwin, P. S., and Hibbard, K.  
13 A.: A Global Terrestrial Monitoring Network Integrating Tower Fluxes, Flask Sampling,  
14 Ecosystem Modeling and EOS Satellite Data, *Remote Sens. Environ.*, 70, 108–127, 1999.

15 Schmid, H. P.: Source areas for scalars and scalar fluxes, *Boundary-Layer Meteorol.*, 67,  
16 293–318, doi:10.1007/BF00713146, 1994.

17 Serrano, L., Filella, I., and Peñuelas, J.: Remote Sensing of Biomass and Yield of Winter  
18 Wheat under Different Nitrogen Supplies, *Crop Sci.*, 40, 723–731, 2000.

19 Sims, D. A. and Gamon, J. A.: Relationships between leaf pigment content and spectral  
20 reflectance across a wide range of species, leaf structures and developmental stages, *Remote*  
21 *Sens. Environ.*, 81, 337–354, doi:10.1016/S0034-4257(02)00010-X, 2002.

22 Sims, D. A., Luo, H., Hastings, S., Oechel, W. C., Rahman, A. F., and Gamon, J. A.: Parallel  
23 adjustments in vegetation greenness and ecosystem CO<sub>2</sub> exchange in response to drought in a  
24 Southern California chaparral ecosystem, *Remote Sens. Environ.*, 103, 289–303,  
25 doi:10.1016/j.rse.2005.01.020, 2006.

26 Sims, D., Rahman, a, Cordova, V., Elmasri, B., Baldocchi, D., Bolstad, P., Flanagan, L.,  
27 Goldstein, a, Hollinger, D. and Misson, L.: A new model of gross primary productivity  
28 for North American ecosystems based solely on the enhanced vegetation index  
29 and land surface temperature from MODIS, *Remote Sens. Environ.*, 112(4), 1633–1646,  
30 doi:10.1016/j.rse.2007.08.004, 2008.

1 Sjöström, M., Ardö, J., Eklundh, L., El-Tahir, B. A., El-Khidir, H. A. M., Hellström, M.,  
2 Pilesjö, P., and Seaquist, J.: Evaluation of satellite based indices for gross primary production  
3 estimates in a sparse savanna in the Sudan, *Biogeosciences*, 6, 129–138, 2009.

4 Stenberg, P., Rautiainen, M., Manninen, T., Voipio, P., and Smolander, H.: Reduced Simple  
5 Ratio Better than NDVI for Estimating LAI in Finnish Pine and Spruce Stands, *Silva Fenn.*,  
6 38(1), 3–14, 2004.

7 Vescovo, L. and Gianelle, D.: Mapping the green herbage ratio of grasslands using both aerial  
8 and satellite-derived spectral reflectance, *Agric. Ecosyst. Environ.*, 115, 141–149,  
9 doi:10.1016/j.agee.2005.12.018, 2006.

10 Vescovo, L. and Gianelle, D.: Using the MIR bands in vegetation indices for the estimation of  
11 grassland biophysical parameters from satellite remote sensing in the Alps region of Trentino  
12 (Italy), *Adv. Sp. Res.*, 41, 1764–1772, doi:10.1016/j.asr.2007.07.043, 2008.

13 Vescovo, L., Wohlfahrt, G., Balzarolo, M., Pilloni, S., Sottocornola, M., Rodeghiero, M., and  
14 Gianelle, D.: New spectral vegetation indices based on the near-infrared shoulder wavelengths  
15 for remote detection of grassland phytomass, *Int. J. Remote Sens.*, 33(7), 2178–2195, 2012.

16 Viña, A., Gitelson, A. A., Nguy-Robertson, A. L., and Peng, Y.: Comparison of different  
17 vegetation indices for the remote assessment of green leaf area index of crops, *Remote Sens.*  
18 *Environ.*, 115, 3468–3478, doi:10.1016/j.rse.2011.08.010, 2011.

19 Walter-Shea, E. A., Privette, J., Cornell, D., Mesarch, M. A., and Hays, C. J.: Relations  
20 between Directional Spectral Vegetation Indices and Leaf Area and Absorbed Radiation in  
21 Alfalfa, *Remote Sens. Environ.*, 61, 162–177, 1997.

22 Wohlfahrt, G., Pilloni, S., Hörtnagl, L., and Hammerle, A.: Estimating carbon dioxide fluxes  
23 from temperate mountain grasslands using broad-band vegetation indices, *Biogeosciences*, 7,  
24 683–694 [online] Available from: [http://www.pubmedcentral.nih.gov/articlerender.fcgi?artid=](http://www.pubmedcentral.nih.gov/articlerender.fcgi?artid=3856878&tool=pmcentrez&rendertype=abstract)  
25 [3856878&tool=pmcentrez&rendertype=abstract](http://www.pubmedcentral.nih.gov/articlerender.fcgi?artid=3856878&tool=pmcentrez&rendertype=abstract), 2010.

26 Wu, C., Niu, Z., Tang, Q., and Huang, W.: Estimating chlorophyll content from hyperspectral  
27 vegetation indices: modeling and validation, *Agric. For. Meteorol.*, 148, 1230–1241,  
28 doi:10.1016/j.agrformet.2008.03.005, 2008.

- 1 Wu, C., Niu, Z., Tang, Q., Huang, W., Rivard, B., and Feng, J.: Remote estimation of gross  
2 primary production in wheat using chlorophyll-related vegetation indices, *Agric. For.*  
3 *Meteorol.*, 149, 1015–1021, doi:10.1016/j.agrformet.2008.12.007, 2009.
- 4 Xiao, X., Zhang, Q., Braswell, B., Urbanski, S., Boles, S., Wofsy, S., Moore III, B., and  
5 Ojima, D.: Modeling gross primary production of temperate deciduous broadleaf forest  
6 using satellite images and climate data, *Remote Sens. Environ.*, 91, 256–270,  
7 doi:10.1016/j.rse.2004.03.010, 2004.
- 8 Zarco-Tejada, P. J., Miller, J. R., Noland, T. L., Mohammed, G. H., and Sampson, P. H.:  
9 Scaling-up and model inversion methods with narrowband optical indices for chlorophyll  
10 content estimation in closed forest canopies with hyperspectral data, *IEEE Trans. Geosci.*  
11 *Remote Sens.*, 39(7), 1491–1507, doi:10.1109/36.934080, 2001.

1 Table 1. Multispectral Cropsan MSR16R system specifications.

Cropsan Multispectral Radiometer (MSR16R)			
Band number	Channel name	Center wavelength (nm)	Bandwidth (nm)
1	R470	469.0	8.8
2	R531	531.1	8.0
3	R547	546.7	8.7
4	R570	569.6	10.4
5	R610	610.1	9.3
6	R640	639.8	10.0
7	R681	681.4	10.7
8	R720	720.2	9.6
9	R730	730.4	10.2
10	R750	749.5	10.6
11	R781	781.0	9.8
12	R861	861.4	10.5
13	R902	901.6	8.7
14	R979	979.1	10.2
15	R1238	1238.0	10.6
16	R1660	1659.8	14.4

1 Table 2. Spectral vegetation indices presented in this study: Normalized Difference  
 2 Vegetation Index, NDVI; Modified Simple Ratio, MSR; Difference Ratio, DR; Red-Edge  
 3 Normalized Difference Vegetation Index, NDVI<sub>red-edge</sub>; Chlorophyll Index, CI<sub>red-edge</sub>. R refers  
 4 to the reflectance at a specific band (nm).

Index	Formulation	Reference
NDVI	$(R_{750}-R_{681})/(R_{750}+R_{681})$	Rouse et al. (1973)
MSR	$(R_{750}/R_{681}-1)/(R_{750}/R_{681}+1)^{1/2}$	Haboudane et al. (2004)
DR	$(R_{750}-R_{720})/(R_{750}-R_{681})$	Datt (1999)
NDVI <sub>red-edge</sub>	$(R_{750}-R_{720})/(R_{750}+R_{720})$	Gitelson and Merzlyak (1994)
CI <sub>red-edge</sub>	$(R_{750}/R_{720})-1$	Gitelson et al. (2003a)

1 Table 3. The four models for  $GEP_m$  estimation tested in the presented study.

Model	Model formulation:
1	$GEP_m = b_0 + b_1 VI$
2	$GEP_m = b_0 + b_1 (VI \cdot PAR_m)$
3	$GEP_m = b_0 + b_1 R470 + b_2 R531 + b_3 R547 + b_4 R570 + b_5 R610 + b_6 R640 + b_7 R681 + b_8 R720 + b_9 R730 + b_{10} R750 + b_{11} R781 + b_{12} R861 + b_{13} R902 + b_{14} R979$
4	$GEP_m = b_0 + b_1 R470 + b_2 R531 + b_3 R547 + b_4 R570 + b_5 R610 + b_6 R640 + b_7 R681 + b_8 R720 + b_9 R730 + b_{10} R750 + b_{11} R781 + b_{12} R861 + b_{13} R902 + b_{14} R979 + b_{15} PAR_m$

1 Table 4. Summary of the statistics ( $n$ -number of observations,  $adjR^2$ -adjusted coefficient of determination, RMSE-root mean square error,  
 2 PRMSE-percentage root mean square error) of the two linear regression models tested in this study both annually, and considering all of the  
 3 five observation years together. The 3 best-fitting models in each group are printed in bold. The best performing model is additionally  
 4 highlighted in italic. All the regressions were statistically significant ( $p < 0.01$ ).

Model	VIs	Meteo data	2008				2009				2010				2011				2012				2008-2012			
			$n$	$adjR^2$	RMSE	PRMSE	$n$	$adjR^2$	RMSE	PRMSE	$n$	$adjR^2$	RMSE	PRMSE	$n$	$adjR^2$	RMSE	PRMSE	$n$	$adjR^2$	RMSE	PRMSE	$n$	$adjR^2$	RMSE	PRMSE
			-	-	$\mu\text{mol m}^{-2}\text{s}^{-1}$	%	-	-	$\mu\text{mol m}^{-2}\text{s}^{-1}$	%	-	-	$\mu\text{mol m}^{-2}\text{s}^{-1}$	%	-	-	$\mu\text{mol m}^{-2}\text{s}^{-1}$	%	-	-	$\mu\text{mol m}^{-2}\text{s}^{-1}$	%	-	-	$\mu\text{mol m}^{-2}\text{s}^{-1}$	%
1	NDVI	-		0.65	3.97	22.95	<b>0.80</b>	<b>3.12</b>	<b>14.88</b>		0.64	3.71	18.50		0.53	3.70	15.16		0.63	3.40	15.36		0.63	4.07	19.57	
	MSR	-		<b>0.70</b>	<b>3.66</b>	<b>21.16</b>	<b>0.81</b>	<b>3.09</b>	<b>14.72</b>		<b>0.68</b>	<b>3.53</b>	<b>17.59</b>		0.50	3.80	15.57		0.66	3.24	14.65		0.64	4.04	19.43	
	DR	-	116	0.60	4.23	24.43	139	0.74	3.59	17.12	123	0.64	3.72	18.55	88	<b>0.64</b>	<b>3.22</b>	<b>13.20</b>	107	<b>0.77</b>	<b>2.66</b>	<b>12.05</b>	573	<b>0.67</b>	<b>3.87</b>	<b>18.64</b>
	NDVI <sub>red-edge</sub>	-		<b>0.70</b>	<b>3.66</b>	<b>21.14</b>	<b>0.81</b>	<b>3.04</b>	<b>14.49</b>		<b>0.69</b>	<b>3.45</b>	<b>17.20</b>		<b>0.61</b>	<b>3.37</b>	<b>13.80</b>		<b>0.80</b>	<b>2.50</b>	<b>11.29</b>		<b>0.74</b>	<b>3.41</b>	<b>16.40</b>	
	CI <sub>red-edge</sub>	-		<b>0.71</b>	<b>3.59</b>	<b>20.76</b>	0.76	3.48	16.58		<b>0.68</b>	<b>3.50</b>	<b>17.47</b>		<b>0.61</b>	<b>3.36</b>	<b>13.74</b>		<b>0.81</b>	<b>2.46</b>	<b>11.10</b>		<b>0.73</b>	<b>3.47</b>	<b>16.72</b>	
2	NDVI	PAR <sub>m</sub>		0.55	4.49	25.96	0.41	5.40	25.76		0.40	4.81	23.98		0.55	3.60	14.73		0.28	4.75	21.49		0.47	4.90	23.58	
	MSR	PAR <sub>m</sub>		<b>0.62</b>	<b>4.14</b>	<b>23.94</b>	<b>0.53</b>	<b>4.84</b>	<b>23.07</b>		<b>0.64</b>	<b>3.73</b>	<b>18.59</b>		<b>0.66</b>	<b>3.14</b>	<b>12.86</b>		<b>0.59</b>	<b>3.60</b>	<b>16.29</b>		<b>0.60</b>	<b>4.24</b>	<b>20.43</b>	
	DR	PAR <sub>m</sub>	116	0.50	4.75	27.47	139	0.40	5.47	26.07	123	0.38	4.88	24.33	88	0.32	4.42	18.09	107	0.18	5.07	22.91	573	0.41	5.13	24.71
	NDVI <sub>red-edge</sub>	PAR <sub>m</sub>		<b>0.65</b>	<b>3.96</b>	<b>22.89</b>	<b>0.56</b>	<b>4.69</b>	<b>22.36</b>		<b>0.60</b>	<b>3.92</b>	<b>19.52</b>		<b>0.61</b>	<b>3.38</b>	<b>13.82</b>		<b>0.42</b>	<b>4.25</b>	<b>19.21</b>		<b>0.61</b>	<b>4.19</b>	<b>20.18</b>	
	CI <sub>red-edge</sub>	PAR <sub>m</sub>		<b>0.68</b>	<b>3.79</b>	<b>21.89</b>	<b>0.60</b>	<b>4.46</b>	<b>21.30</b>		<b>0.70</b>	<b>3.38</b>	<b>16.83</b>		<b>0.66</b>	<b>3.12</b>	<b>12.79</b>		<b>0.57</b>	<b>3.67</b>	<b>16.60</b>		<b>0.67</b>	<b>3.87</b>	<b>18.65</b>	

1 Table 5. Summary of the general multiple regressions: partial adjusted  $R^2$ , variance inflation  
 2 factor (VIF), significance levels of the predictor variables ( $p$ ), number of observations ( $n$ ),  
 3 cumulative adjusted  $R^2$ , root mean square error (RMSE) and percentage root mean square  
 4 error (PRMSE). R - refers to reflectance at a given waveband (e.g. R720 - reflectance at 720  
 5 nm).

Model	Explanatory variables	partial adjusted $R^2$	VIF	$p$	$n$	cumulative adjusted $R^2$	RMSE	PRMSE
3	R681	0.44	5.65	0.00412	573	0.73	3.50	16.83
	R781	0.26	3.54	< 2e-16				
	R720	0.04	6.78	< 2e-16				
4	R681	0.44	5.69	0.0323	573	0.79	3.06	14.75
	R781	0.26	6.74	< 2e-16				
	PAR <sub>m</sub>	0.07	1.25	< 2e-16				
	R720	0.03	7.25	2.60E-16				



1 Table 6. Summary of the statistical metrics of gap filling procedure: adjusted  $R^2$  ( $\text{adj}R^2$ ), root  
 2 mean square error (RMSE) and percentage root mean square error (PRMSE).

Model		Gap length								
		1 observation day			3 observation days			5 observation days		
		$\text{adj}R^2$	RMSE	PRMSE	$\text{adj}R^2$	RMSE	PRMSE	$\text{adj}R^2$	RMSE	PRMSE
	-	$\mu\text{molm}^{-2}\text{s}^{-1}$	%	-	$\mu\text{molm}^{-2}\text{s}^{-1}$	%	-	$\mu\text{molm}^{-2}\text{s}^{-1}$	%	
1	mean	0.76	3.41	16.45	0.72	3.43	16.71	0.70	3.34	16.28
	range	0.16	0.73	3.80	0.28	1.19	5.45	0.46	0.95	6.50
4	mean	0.78	3.16	15.25	0.77	3.10	15.08	0.73	3.17	15.42
	range	0.14	0.46	2.72	0.18	0.81	4.23	0.33	0.75	5.13

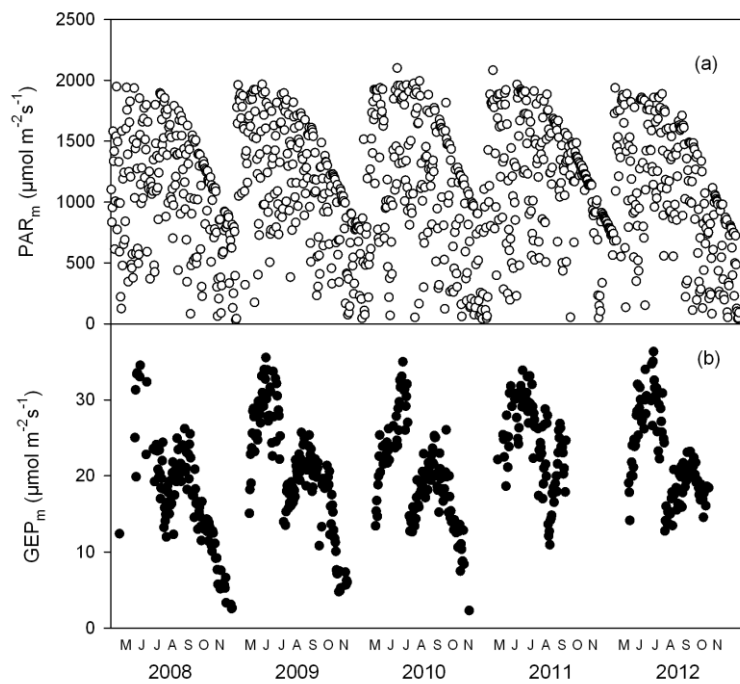
1 Table A1. Spectral vegetation indices investigated in this study. R refers to the reflectance at a  
 2 specific band (nm).

Index	Formulation	Reference
NDVI	$(R750-R681)/(R750+R681)$	Rouse et al. (1973)
	$(R781-R681)/(R781+R681)$	
	$(R861-R681)/(R861+R681)$	
	$(R750-R547)/(R750+R547)$	
NDVI <sub>green</sub>	$(R781-R547)/(R781+R547)$	Gitelson et al. (1996)
	$(R861-R547)/(R861+R547)$	
SR	R750/R681	Jordan (1969)
	R781/R681	
	R861/R681	
SR <sub>green</sub>	R750/R547	Gitelson and Merzlyak (1997)
	R781/R547	
	R861/R547	
SR <sub>blue</sub>	R470/R750	Zarco-Tejada et al. (2001)
	R470/R781	
MSR	R470/R861	Haboudane et al. (2004)
	$(R750/R681-1)/(R750/R681+1)^{1/2}$	
	$(R781/R681-1)/(R781/R681+1)^{1/2}$	
RDVI	$(R861/R681-1)/(R861/R681+1)^{1/2}$	Haboudane et al. (2004)
	$(R750-R681)/(R750+R681)^{1/2}$	
	$(R781-R681)/(R781+R681)^{1/2}$	
NDVI <sub>red-edge</sub>	$(R861-R681)/(R861+R681)^{1/2}$	Gitelson and Merzlyak (1994)
	$(R750-R720)/(R750+R720)$	
MTCI	$(R781-R720)/(R781+R720)$	Dash and Curran (2004)
	$(R861-R720)/(R861+R720)$	
	$(R750-R720)/(R720-R681)$	

	$(R781-R720)/(R720-R681)$	
	$(R861-R720)/(R720-R681)$	
	$2.5*(R750-R681)/(1+R750+6*R681-7.5*R470)$	
EVI	$2.5*(R781-R681)/(1+R781+6*R681-7.5*R470)$	Huete et al. (2002)
	$2.5*(R861-R681)/(1+R861+6*R681-7.5*R470)$	
	$(R750/R720)-1$	
CI <sub>red-edge</sub>	$(R781/R720)-1$	Gitelson et al. (2003a)
	$(R861/R720)-1$	
	$(R750/R720)-1$	
CI <sub>green</sub>	$(R781/R720)-1$	Gitelson et al. (2003c)
	$(R861/R720)-1$	
	$(R547-R531)/(R547+R531)$	
	$(R570-R531)/(R570+R531)$	
PRI	$(R610-R531)/(R610+R531)$	Gamon et al. (1992)
	$(R640-R531)/(R640+R531)$	
	$(R681-R531)/(R681+R531)$	
	$(R750-R470)/(R720-R470)$	
mSR	$(R781-R470)/(R720-R470)$	Sims and Gamon (2002)
	$(R861-R470)/(R720-R470)$	
	$(R750-R720)/(R750-R681)$	
DR	$(R781-R720)/(R781-R681)$	Datt (1999)
	$(R861-R720)/(R861-R681)$	
	$(R750-R720)/(R750+R720-2R470)$	
mND	$(R781-R720)/(R781+R720-2R470)$	Sims and Gamon (2002)
	$(R861-R720)/(R861+R720-2R470)$	
	$(R750-R681)/(R750+R681-2R470)$	
mNDVI	$(R781-R681)/(R781+R681-2R470)$	Main et al. (2011)
	$(R861-R681)/(R861+R681-2R470)$	
VOG	R730/R720	Zarco-Tejada et al. (2001)

	$(R750-R470)/(R750-R681)$	
SIPI	$(R781-R470)/(R781-R681)$	Peñuelas et al. (1995)
	$(R861-R470)/(R861-R681)$	
	$(R750-R547)/(R750-R681)$	
SIPI 2	$(R781-R547)/(R781-R681)$	Blackburn (1998)
	$(R861-R547)/(R861-R681)$	
MCARI	$[(R720-R681)-0.2*(R720-R547)](R720/R681)$	Daughtry et al. (2000)
	$[(R750-R720)-0.2*(R750-R547)](R750/R720)$	
MCARI 2	$[(R781-R720)-0.2*(R781-R547)](R781/R720)$	Wu et al. (2008)
	$[(R861-R720)-0.2*(R861-R547)](R861/R720)$	
	$(0.1*R750-R681)/(0.1*R750+R681)$	
WDRVI	$(0.1*R781-R681)/(0.1*R781+R681)$	Gitelson (2004)
	$(0.1*R861-R681)/(0.1*R861+R681)$	
	$(R781-R750)$	
ISI	$(R861-R750)$	Vescovo et al. (2012)
	$(R781-R750)/(R781+R750)$	
NIDI	$(R861-R750)/(R861+R750)$	Vescovo et al. (2012)
	$(R781-R750)/(R781+R750)$	
WBI	R979/R902	Peñuelas et al. (1994)

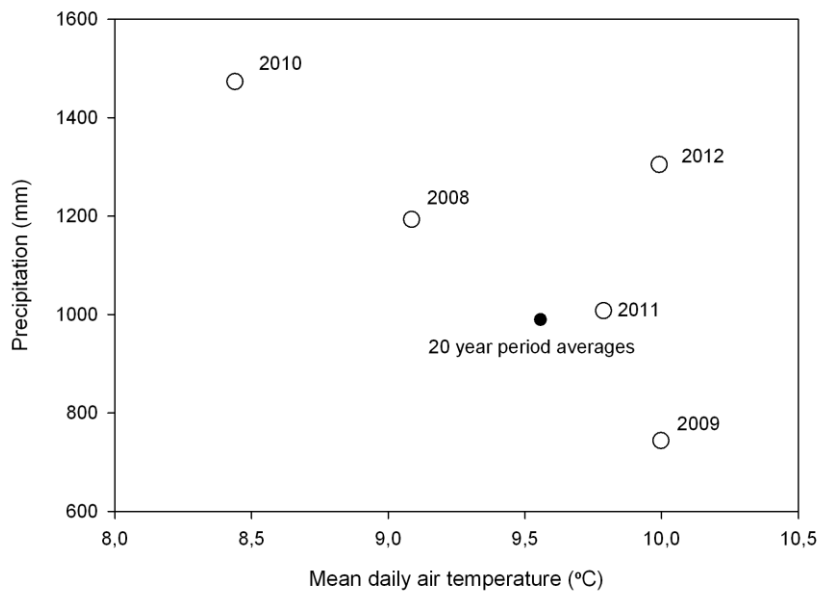
---



1

2

3 Figure 1. Seasonal variation of: (a) mean midday PAR ( $\text{PAR}_m$ ;  $\mu\text{mol m}^{-2} \text{s}^{-1}$ ), (b) mean  
 4 midday GEP ( $\text{GEP}_m$ ;  $\mu\text{mol m}^{-2} \text{s}^{-1}$ ) in the growing seasons of 2008-2012.

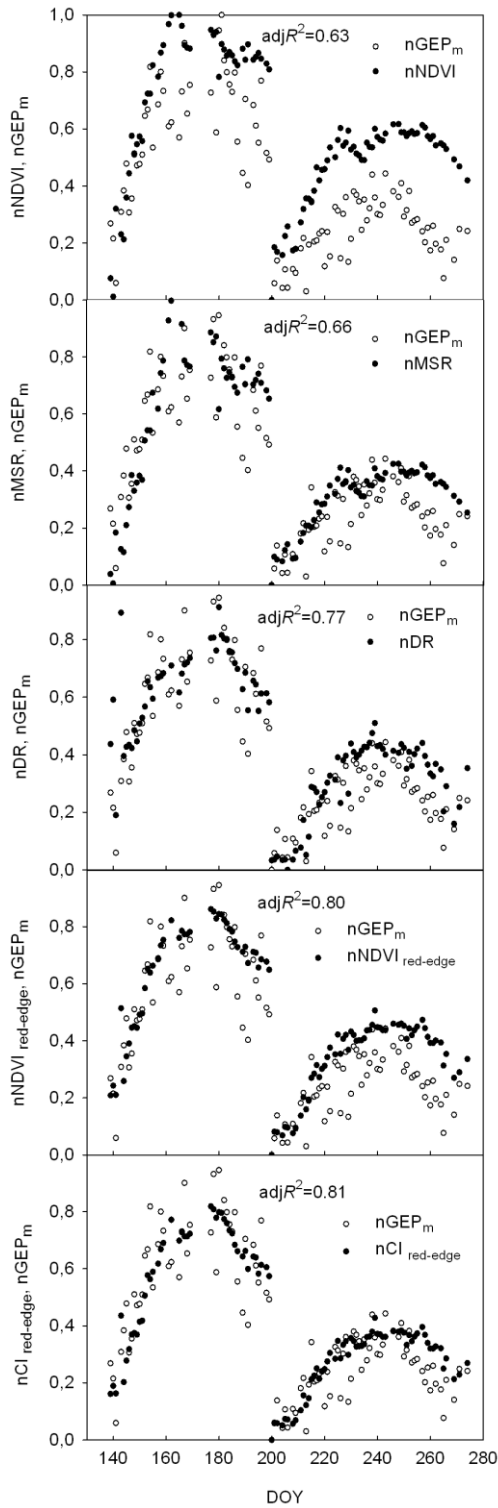


1

2

3 Figure 2. Cumulative precipitation versus average daily air temperature for the period May-

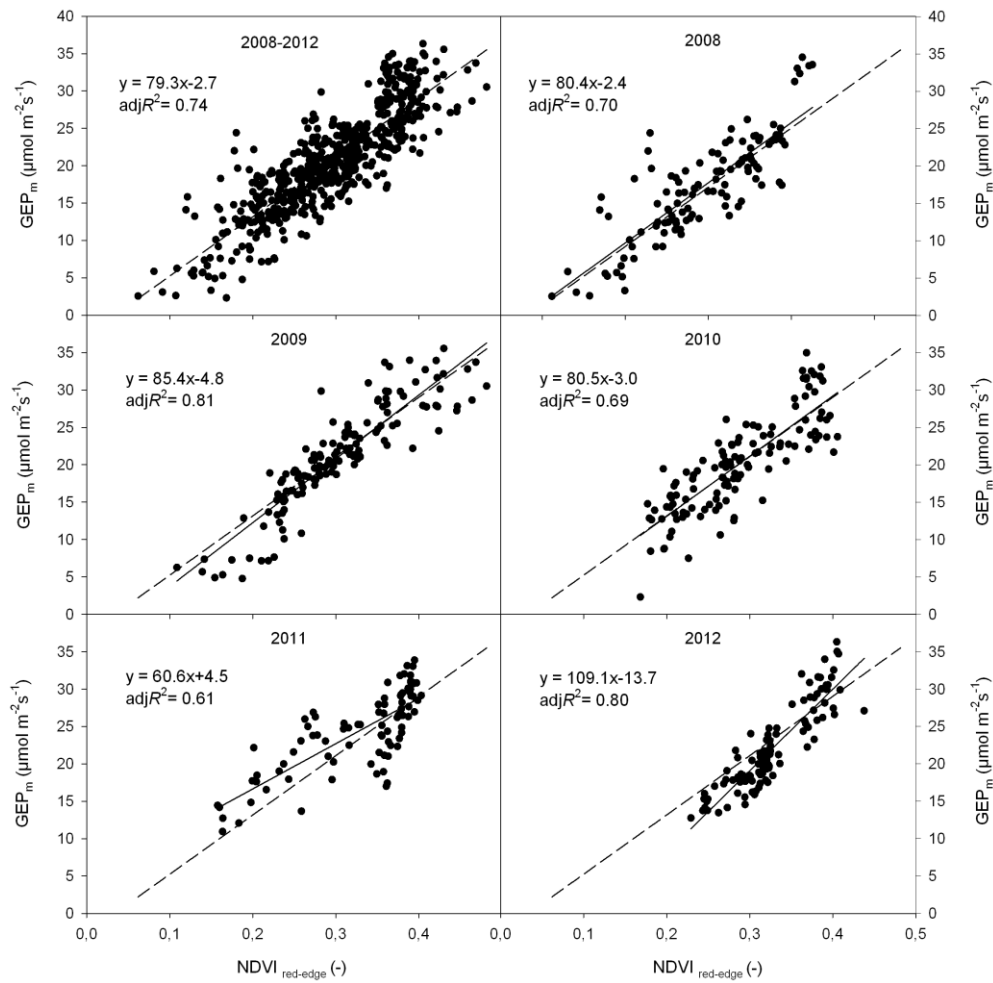
4 November.



1

2

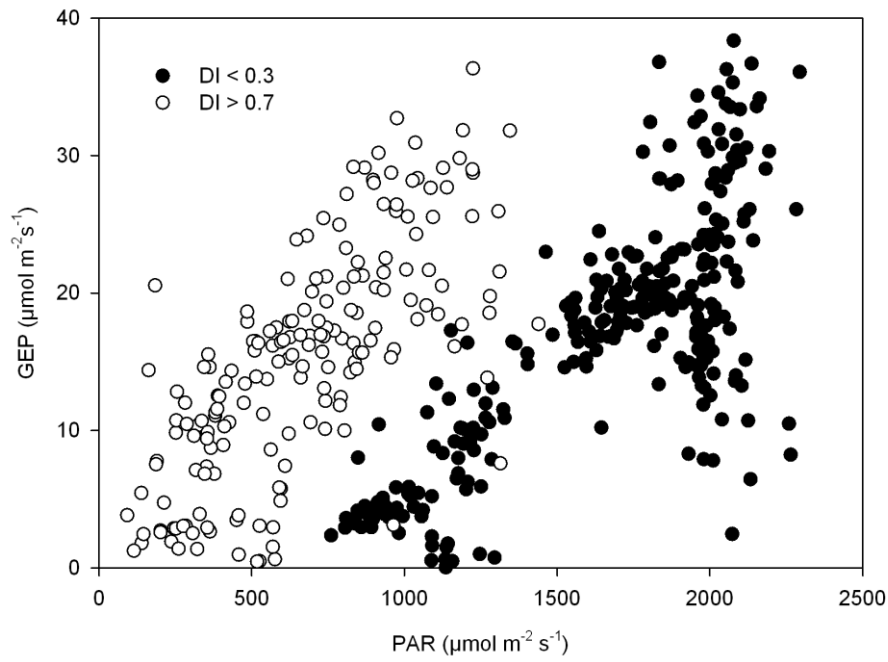
3 Figure 3. Seasonal courses of normalized spectral vegetation indices - nVIs (-) and  
 4 normalized mean midday gross ecosystem production - nGEP<sub>m</sub> (-) in the growing season of  
 5 2012;  $adjR^2$  between GEP<sub>m</sub> estimated from EC measurements and GEP<sub>m</sub> obtained with model  
 6 1 fed with the various VIs.



1  
2

3 Figure 4. Relationship between the Red-Edge Normalized Difference Vegetation Index  
 4 ( $NDVI_{red-edge}$ ) and mean midday gross ecosystem production ( $GEP_m$ ), considering both the 5  
 5 years of observation together and annual observations. Dashed and solid trend lines refer to  
 6 the general model 1 (considering each year of observation) and model 1 based on the  
 7 observations from a specific year, respectively.

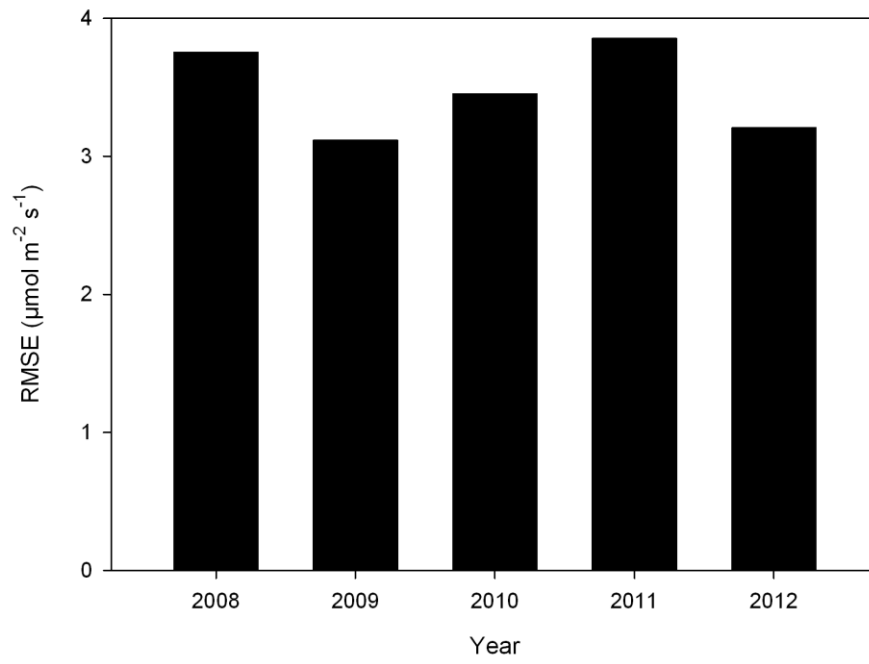




1

2

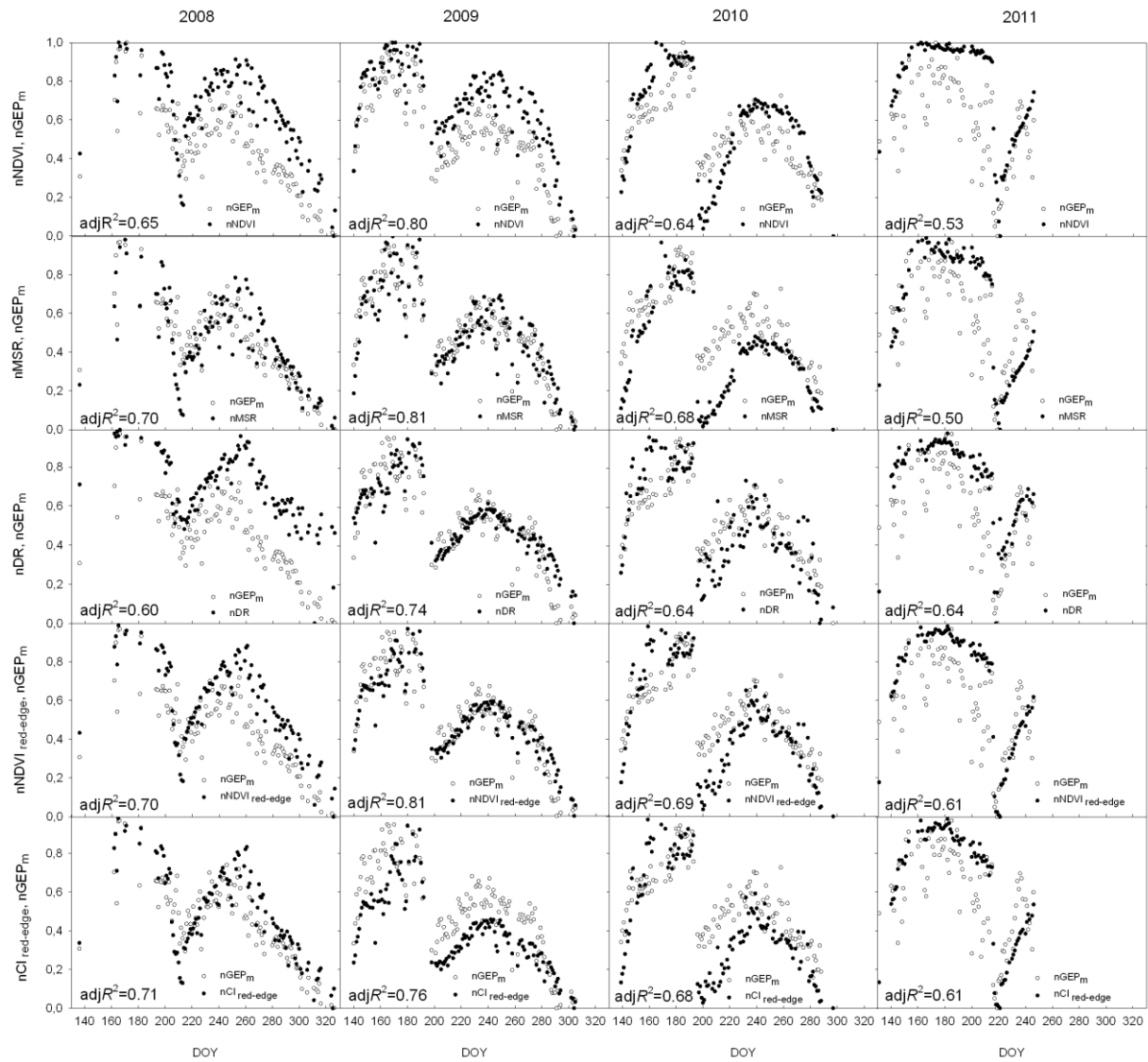
3 Figure 5. Light response of half-hourly gross ecosystem production (GEP; from 11:00 a.m. to  
4 1:00 p.m.) to the incident photosynthetically active radiation (PAR) in the snow-free period of  
5 2012 (May-November). Diffusion index (DI) is the ratio between diffuse and total incident  
6 PAR. It ranges from 0 to 1.



1

2

3 Figure 6. Root mean square error (RMSE) of the validated models based on the Red-Edge  
4 Normalized Difference Vegetation Index ( $\text{NDVI}_{\text{red-edge}}$ ).



1

2

3 Figure B1. Seasonal courses of normalized spectral vegetation indices - nVIs (-) and  
 4 normalized mean midday gross ecosystem production - nGEP<sub>m</sub> (-) in the growing seasons of  
 5 2008-2011 (left-right panel); adjR<sup>2</sup> between GEP<sub>m</sub> estimated from EC measurements and  
 6 GEP<sub>m</sub> obtained with model 1 fed with the various VIs.